



SIMULATIVE AND REAL TIME DC MOTOR SPEED CONTROL

AHMED IMADMAHMOOD

AUGUST 2016

SIMULATIVE AND REAL TIME DC MOTOR SPEED CONTROL

**A THESIS SUBMITTED TO
THE GRADUATE SCHOOL OF NATURAL AND APPLIED
SCIENCES OF
ÇANKAYA UNIVERSITY**

**BY
AHMED IMADMAHMOOD**

**IN PARTIAL FULFILLMENT OF THE REQUIREMENTS FOR THE
DEGREE OF
MASTER OF SCIENCE
IN
THE DEPARTMENT OF
ELECTRONIC AND COMMUNICATION ENGINEERING**

AUGUST 2016

Title of the Thesis **SIMULATIVE AND REAL TIME DC MOTOR SPEED CONTROL**


Submitted by **AHMED IMAD MAHMOOD**

Approval of the Graduate School of Natural and Applied Sciences, Çankaya University.




Prof. Dr. Halil Tanyer EYYUBOĞLU
Director

I certify that this thesis satisfies all the requirements as a thesis for the degree of Master of Science.



Prof. Dr. Yusuf Ziya UMUL
Head of Department

This is to certify that we have read this thesis and that in our opinion it is fully adequate, in scope and quality, as a thesis for the degree of Master of Science.

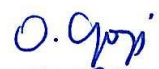



Asst. Prof. Dr. Ulaş BELDEK
Supervisor


Examination Date: 19.08.2016

Examining Committee Members

Assoc. Prof. Dr. Orhan GAZİ (Çankaya Univ.)
Asst. Prof. Dr. Ulaş BELDEK (Çankaya Univ.)
Asst. Prof. Dr. Tolga İNAN (TED Univ.)







STATEMENT OF NON-PLAGIARISM PAGE

I hereby declare that all information in this document has been obtained and presented in accordance with academic rules and ethical conduct. I also declare that, as required by these rules and conduct, I have fully cited and referenced all material and results that are not original to this work.

Name, Last Name : Ahmed Mahmood

Signature :



Date : 19.08.2016

ABSTRACT

SIMULATIVE AND REAL TIME DC MOTOR SPEED CONTROL

AHMED IMAD MAHMOOD

M.Sc., Department of Electronic and Communication Engineering

Supervisor: Assist. Prof. Dr. Ulaş BELDEK

August 2016, 52 pages

DC motor velocity control is one of the most commonly encountered control applications in literature as DC machines are exclusively used in industrial applications. The DC motors are assumed to have linear and stable characteristics, and for this reason, they are supposed to be controlled easily. However, that is not the case in real time applications. This thesis provides a real time controller design approach in cooperation with system identification. Primarily the linear mathematical model of an experimental DC motor speed control system set-up is constructed in simulation and this model is used to obtain a controller for the speed control mission but the controller obtained in the simulation turn out to be unsuccessful in the real time application. Hence, a real time system identification step is executed to attain an approximate system linear model and it is observed that identified system structure varied from the mathematical model significantly. Finally, A new controller is designed for the identified system and it verified by different tests that this controller operates comparably well in real time applications.

Keywords: DC Motor Control, PID Controller, System Identification, Root Locus

ÖZ

DC motor hız kontrolü, DC makineler endüstriyel uygulamalarda sıklıkla kullanıldığından, literatürde en sık karşılaşılan kontrol problemlerindedir. DC motorların doğrusal ve kararlı karaktere sahip oldukları varsayılır ve bu nedenle kontrollerinin kolaylıkla yapılabileceği zannedilir. Buna karşın gerçek zamanlı uygulamalarda bu önerme tam anlamıyla doğru değildir. Bu tez sistem tanımlamayla işbirliği içinde gerçek zamanlı bir denetleyici tasarımı yaklaşımını sunmaktadır. İlk olarak deneysel DC motor hız kontrolü sistemi düzeneğinin matematiksel modeli benzetimde oluşturulmuştur ve bu model hız kontrolü görevi için denetleyici tasarımında kullanılmıştır. Fakat benzetimde elde edilen denetleyici gerçek zamanlı uygulamada başarısız olmuştur. Bu nedenle yaklaşık sistemin doğrusal modelini elde etmek için gerçek zamanlı bir sistem tanımlama adımı uygulanmıştır ve tanımlanan sistemin yapısının matematiksel modelden belirgin şekilde farklı olduğu gözlemlenmiştir. Son olarak, tanımlanan sistem için yeni bir denetleyici tasarlanmış ve bu denetleyicinin gerçek zamanlı uygulamalarda kıyaslanabilir şekilde daha iyi çalıştığı farklı testlerle gösterilmiştir.

Anahtar kelimeler:DC Motor Kontrolü, Oransal-Entegral -Türevsel Denetleyici, Sistem Tanılama, Yer Kök Eğrisi.

DEDICATION

I would like to dedicate this dissertation to the first person and best friend of my life (Imad) my father.

I dedicate this dissertation to the most beautiful woman in the world, my heaven (Sudad) my mother.

I dedicate this dissertation to heart and life (Hannadi) my wife.

I dedicate this dissertation to my dear brother (Ali) and sister (Zumord).

I dedicate this dissertation to my uncle (Nowzad) for his support and encouragement.

I dedicated this dissertation to my aunt (Ashwaq) for her support and encouragement.

ACKNOWLEDGEMENTS

I would like to express my heartfelt gratitude in the completion of this research to my Supervisor Asst. Prof. Dr. Ulaş BELDEK, for his special guidance suggestions, supports and encouragement during the period my thesis. I am indebted for his suggestions and allocating me a lot of time, his patience and willingness to guide me will never be forgotten.

I would like to express my heartfelt gratitude to my wife Hannadi Nowzad for her support and encouragement.

I would like to express my heartfelt gratitude to my friend Salim Abdullah for his helping

I would like to express my heartfelt gratitude to my nephews Ayad, Yasser for their helping.

TABLE OF CONTENTS

STATEMENT OF NON PLAGIARISM	iii
ABSTRACT	iv
ÖZ	v
DEDICATION	vi
ACKNOWLEDGEMENTS	vii
TABLE OF CONTENT	viii
TABLE OF CONTENTS	ix
LIST OF FIGURES	x
LIST OF FIGURES	xi
LIST OF FIGURES	xii
LIST OF TABELS	xiii

CHAPTERS:

1. INTRODUCTION	1
1. 1. Background	1
1. 2. Organization of the Thesis	4
2. DC Motor Control System, PID controllers	5
2. 1. DC Motor Control System	6
2. 2. System Mathematic Model	7
2. 3. PID Controller	11
3. Simulations	12
3. 1. Simulation Model	12
3. 2. Proportional Control with Root Locus	13
3. 3. Proportiona Integral Control with Root Locus	16
4. Real Time Applications	29
4. 1. Methodolgy	29
4. 2. Test of the Developed Simulation Model Controller in Rea	ITime
applicatio	29

4.3. System Identification	31
4.3.1. System Identification with Sinusoidal and Random Signal	32
4.4. Proportiona Integral Control with Root Locus	34
4.5. Controller Design with P controller	44
Conclusion	48
REFERENCES	50



LIST OF FIGURES

Figure 2.1: Precision Modular Servo electrical and mechanical components.....	6
Figure 2.2: Servo motor complete control system	7
Figure 2.3: DC motor mechanical parts	7
Figure 2.4: DC motor model.....	10
Figure 2.5: The sub-block for the DC motor model.....	11
Figure 2.6: General control system scheme.....	11
Figure 2.7: SIMULINK Control model for DC motor speed control.....	12
Figure 3.1: Root locus transfer function in equation.....	13
Figure 3.2: Velocity profile obtained using the controller structure in equation 3.2 for tracking unit step reference signal of 400 rot/min.....	15
Figure 3.3: Velocity profile (red plot) obtained using the controller structure in equation 3.3 for tracing unit step signal of 400 rot/min (blue plot).....	16
Figure 3.4: Voltage profile when the proportional gain is increased.....	17
Figure 3.5: Root locus plot of equation 3.8.....	19
Figure 3.6: Voltage, velocity, position and current profiles for tracking unit step reference signal of 400 rot/min.....	20
Figure 3.7: Voltage, velocity, external torque and current profiles for unit step reference signal tracking of 400 rot/min.....	21
Figure 3.8: Angular velocity (reference signal) given in Equation 3.1.....	22

Figure 3.9: Velocity profile when pulse type external torque applied while tracking the reference signal given in equation 3.10	22
Figure 3.10: Voltage, velocity, torque and current profiles when pulse type external torque applied while tracking the reference signal given in equation 3.10.....	23
Figure 3.11: Voltage, velocity, external torque and current profiles for sinusoidal reference signal tracking when external torque in equation 4.11 applied.....	24
Figure 3.12: Velocity profile for sinusoidal reference signal tracking when external torque in equation 4.11 is applied.....	24
Figure 3.13: Effect of changing the external disturbance as in equation 3.12 for sinusoidal reference signal tracking.....	25
Figure 3.14: Effect of changing the external disturbance as in equation 3.13 for sinusoidal reference signal tracking	26
Figure 3.15: Voltage, velocity, external torque and current profiles in case of external square torque.....	27
Figure 3.16: Reference and actual velocity profile in case of external square torque.....	27
Figure 3.17: Reference and actual velocity profile with higher resolution in case of external square torque.....	28
Figure 4.1: The real time SIMULINK model	30
Figure 4.2: Desired, actual velocity and voltage signals for real time system using the controller given in equation	31
Figure 4.3: Real time model structure.....	32

Figure 4.4: Root locus plot for the transfer function in Equation 4.3.....	33
Figure 4.5: Root locus plot for Equation 4.8.....	35
Figure 4.6: Voltage and velocity profiles for sinusoidal reference signal tracking using controller in Equation 4.9.....	36
Figure 4.7: Voltage and velocity profiles for square reference signal tracking using controller in Equation 4.9.....	37
Figure 4.8: Voltage and velocity profiles when $p=0.0249$ and $I= 0.001$ for square reference signal tracking.....	39
Figure 4.9: Desired and actual velocity with the effect of sinusoidal reference signal tracking.....	39
Figure 4.10: The real time SIMULINK model with a saturation device (block).....	40
Figure 4.11: Voltage and velocity profiles with the effect of saturation block for sinusoidal reference signal tracking.....	41
Figure 4.12: Voltage and velocity profiles with the effect of saturation block for square signal reference tracking.....	41
Figure 4.13: Voltage and velocity profiles with the effect of magnetic disturbance for square reference signal tracking.....	42
Figure 4.14: Voltage and velocity profiles with the effect of magnetic disturbance for sinusoidal reference signal tracking.....	43

LIST OF TABLE

Table 2.1: DC motor parameters	10
Table 4.1: DC motor velocity, overshoot, steady state error and rise	
Timeresults.....	38



CHAPTER 1

INTRODUCTION

1.1. Background

In today's world, roughly all mechanical processes that we observe around are accomplished by different kinds of electrical motors. For this reason, using experimental set-ups to enable implementing and testing of different control applications [1] is important to increase their practical usage and efficiency. These machines are producers of rotational energy and their principle of operation depends on transforming electrical power to mechanical motion. Subject to the processes they are involved, electrical motors come in different dimensions. Enormous motors might be employed to carry loads of 1000's of Horsepower especially in production processes. Several examples of big motor applications include hoists, road electrical trains, elevators and big rolling mills. Furthermore, medium or small sized motors also have many application areas such as transportation machines, artificial intelligent robots, hand power instruments and food mixers. Besides, due to the development in science and technology, new operational usage fields such as medicine are also opened for these machines. Therefore, electrical motors cover a huge space in our day life. Hence, their properties and characteristics such as efficiency, accessibility and convenience in applications and processes, power density, price and ease of control are vital in daily life to promote high productivity. From this perspective, controlling the speed of electrical motors is one of the most important issues. Speed control of motors faces with various sorts of difficulties such as precision [2] and applicability in altering load conditions [3] hence the design of the control system for speed control should cope with such problems. To deal with the challenges that are encountered during speed control of motors, many control procedures and algorithms are implemented. For this task fuzzy logic [3,4,5,6,7,8] neural-networks [9,10] and machine learning [11,12,13,14] tools are also applicable. However, these tools most of the time are developed off-line and some priori information about the system are necessary to design and implement them.

Nevertheless, in real time applications there are uncertainties about the parameters of the system and hence the system dynamics these methods are applied can be erroneous, Hence most of the time a system identification is necessary to estimate the systems characteristics in real time applications. One of the most convenient and favored control settlements to handle the challenges in control applications is called as proportional-integral-derivative (PID) control[15]. PID controllers are also widely used for speed control of electrical motors [16]. This algorithm is highly preferred as its implementation is easy and as it usually meets the requirements corresponding to the control application by suitable choice of its parameter setting. Hence, the crucial aspect while employing PID controller is the determination of PID controller parameters. If the PID controller parameters are selected appropriately the requirements in the speed control such as tracking different types of reference input signals properly in a short period of time with conceivable smallest overshoot and also with the minimum rate of error as quickly as possible can be satisfied with high efficiency. Additional technique can also assist to determine the parameters of PID controllers. One of these techniques is called as root locus[17, 18]. The technique uses a mathematical function analysis background in order to designate the locations of the closed loop poles of a linear system, which is represented by an open loop transfer function. Evans proposed a modern and simple graphical approach to explain the closed-loop characteristic of the roots of the characteristic equation and for this reason it is called as the root locus. It is a graphical technique for testing how the roots of a structure changes with dissimilarity of definite system parameters. It has been widely used in control engineering and it offers excessive facilities to the engineers working over control and stability of various systems. The technique can be employed to determine the sensitivity of poles of a transfer function to parameters being measured, to define the steadiness of the system, to resolve the rate of damping ratio and naturalistic frequency. In addition if it is coupled with PID control it can also be used to set some of its parameters as well[8]. Thus root locus can be engaged to improve the system performance in control applications and hence it enables the engineers to stabilize and control the systems outputs. Occasionally, we might possess less or contradicting information about the system characteristics and properties to be controlled. Especially the mathematical model representing the

dynamical system concerned might be incomplete, at times also inaccurate and more dangerously erroneous to represent it adequately. These drawbacks generally arise due to insufficient analysis of the dynamical system as well as deficiencies in mathematical modeling and uncertainties in the system parameters. The worst is the case that we got nothing about the system. In these circumstances, the process, which is called as system identification, should be performed deliberately to attain approximate model of the system. In this thesis, the intention is devising a suitable controller structure that is fruitful in DC motor speed control application both in simulation environment and real time application. Primarily, the mathematical model a DC motor control system that is implemented in a well-known laboratory experiment set up is employed in order to design the controller structure to be used for the speed control simulations in MATLAB. To inject the controller with specific properties such as demonstrating better performance criteria in speed control, the capability of root locus technique is appealed. The designed controller is then tested in the simulation environment and its capacity is experienced. However, in real time applications, the performance of the designed controller is experienced to be insufficient and inefficiency in some of the performance criteria is displayed at the outputs. Due to these negative results, a system identification process is also carried out in advance to obtain the approximate model of the system transfer function. It is observed that the transfer function obtained due to system identification deviates from the mathematically modeled system significantly. Due to the system identification outcomes, a new controller is designed to handle speed control practice in real time applications. In the design of the controller similar principles are employed as done for the simulation case. This new controller structure is tested in real time applications and with some simple parameter changes, it is observed that it works properly in diverse circumstances. The main contribution of this thesis is the integration of system identification process with controller design procedure for real time application. The simulation part is just a preparatory step that enables the system identification and controller design for real time application.

1.2. Organization of the Thesis

This thesis contains five chapters: Chapter 1 presents the introduction part. Chapter 2 presents the fundamental information about the DC motor modeling for speed control, feedback control loop, PID controllers and system identification are emphasized. In Chapter 3, a simulative model is implemented in MATLAB for the dealt DC motor speed control application. The mathematical model of the DC motor is used to develop controller structure and for this task means of root locus technique is employed. Later the designed controllers' performance is tested for reference signal tracking and finally the controller's durability is monitored under different loading and disturbance conditions. Chapter 4 is devoted to design of a similar controller structure as in Chapter 3 for the real time speed control application. However different from Chapter 3 it also includes the system identification process applied to the real time system to attain a better approximate model of the real time system that is used in the control design procedure. Chapter 5 presents the concluding remarks and the future work.

CHAPTER 2

DC Motor Control System, PID Controllers

2.1. DC Motor Control System

The DC motor control system consists of electrical and mechanical parts, which contains the DC motor and also supportive components like tachometer/gearbox, input and output Potentiometers, digital encoder and magnetic brake as it is shown in Figure 2.1[1].

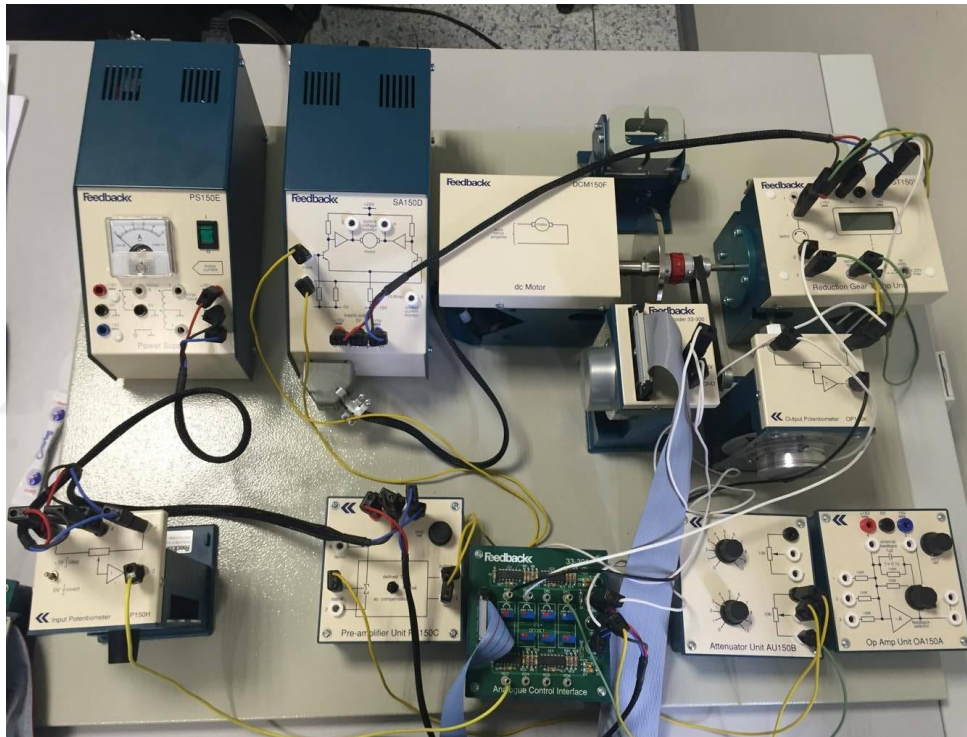


Figure 2.1: Precision Modular Servo electrical and mechanical components

The electrical parts in Figure 2.1 include the electronically manipulated signals responsible for controlling the motor. The measured signals are transferred to the computer via an I/O card. The electrical and mechanical parts create a very complete control system setup as it is shown in Figure 2.2 [1].

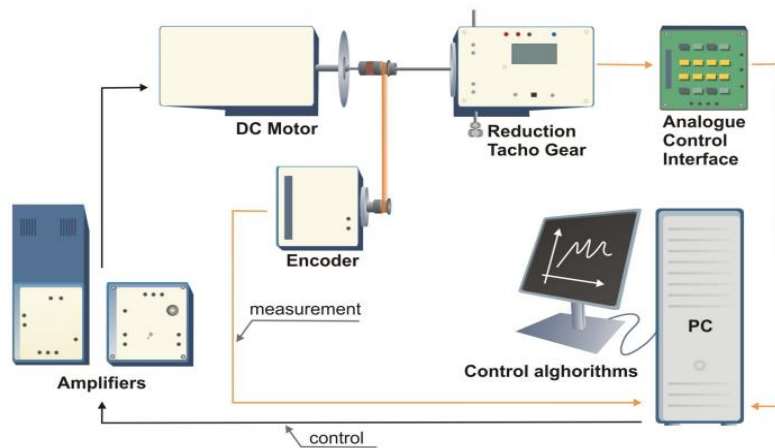


Figure 2.2: Servo motor complete control system [1]

2.2. System Mathematical Model

DC motor main parts are the rotational and fixed parts. Every control project starts with plant modeling. If we decide to design an efficient model, we should know about the process itself. The mechanical parts of the servo motor system is presented in Figure 2.3

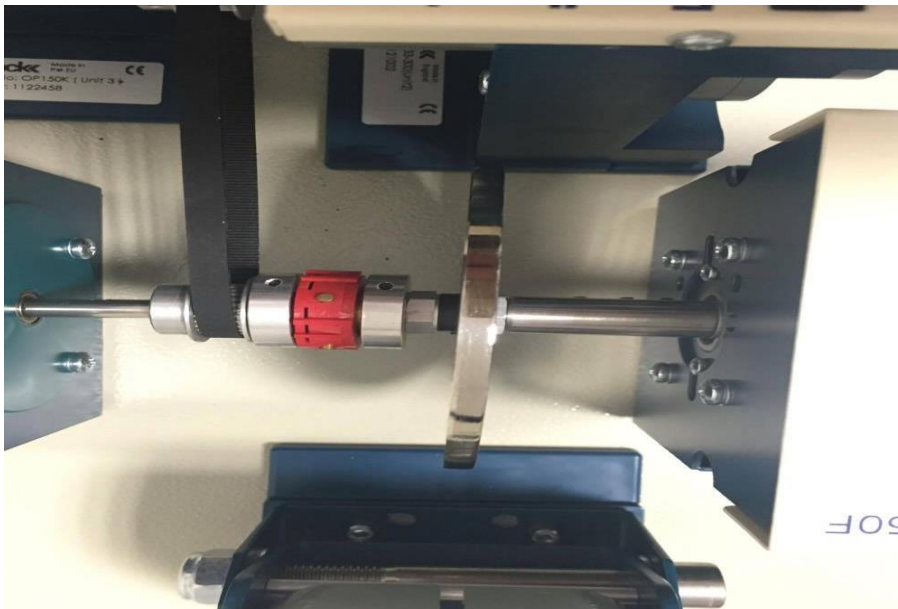


Figure 2.3: DC motor mechanical parts

For a DC motor, the torque induced over the motor is proportional with the current passing from the electrical part. This equation can be written as,

$$\tau = K_t \cdot I \quad (2.1)$$

where K_t is the torque constant for the DC motor, I is the current passing from the electrical part of the motor and τ is the induced torque. Similarly, the back electromotive force induced over the electrical part of the motor is proportion with the angular velocity of the shaft of the motor. This linear equation can be written as

$$V_{emf} = K_b \cdot \dot{\theta} \quad (2.2)$$

where the induced electromotive force is V_{emf} , the electromotive force constant of the motor is K_b , angular velocity of the shaft is $\dot{\theta}$. Using Newton's law, the mechanical dynamic equation can be described by:

$$J\ddot{\theta} = -d\dot{\theta} + \tau - \tau_{ext} = -d\dot{\theta} + K_t \cdot I - \tau_{ext} \quad (2.3)$$

where d is a linear the viscous friction coefficient, J is the moment of inertia of the motor and $\ddot{\theta}$ is the angular acceleration of the motor and τ_{ext} is the load torque (disturbance). Similarly, the electrical equation of the motor can be written as,

$$V_m - V_{emf} = +L \frac{dI}{dt} + R \cdot I \quad (2.4)$$

where V_m is Voltage applied to the armature of the motor, L the inductance value of the armature part of the motor and R is the internal resistance of the armature part. Using Equation 2.2, Equation 2.4 can be transformed into

$$V_m = L \frac{dI}{dt} + R \cdot I + K_b \cdot \dot{\theta} \quad (2.5)$$

Equations 2.3 and 2.5 can be reorganized as a state space representation as,

$$\frac{d}{dt} \begin{bmatrix} \dot{\theta} \\ I \end{bmatrix} = \begin{bmatrix} -\frac{d}{J} & \frac{K_t}{J} \\ -\frac{K_b}{L} & -\frac{R}{L} \end{bmatrix} \cdot \begin{bmatrix} \dot{\theta} \\ I \end{bmatrix} + \begin{bmatrix} 0 \\ \frac{1}{L} \end{bmatrix} \cdot V_m + \begin{bmatrix} -\frac{1}{J} \\ 0 \end{bmatrix} \cdot \tau_{ext} \quad (2.6)$$

We know that the derivative of the angular position θ is equal to angular velocity w ,

$$\dot{\theta} = w \quad (2.7)$$

There are also amplifiers to amplify the signal coming from the computer (between 2.5 Volt and -2.5 Volt) to levels that can be employed to the motor (between 24 Volt and -24 Volt) and this conversion ratio is 9.6. This equation is given by

$$V_m = 9.6 \times u(2.8)$$

Hence, the state-space representation becomes

$$\frac{d}{dt} \begin{bmatrix} W \\ I \end{bmatrix} = \begin{bmatrix} -\frac{d}{J} & \frac{K_t}{J} \\ -\frac{K_b}{L} & -\frac{R}{L} \end{bmatrix} \cdot \begin{bmatrix} W \\ I \end{bmatrix} + \begin{bmatrix} 0 \\ \frac{9.6}{L} \end{bmatrix} \cdot u + \begin{bmatrix} -\frac{1}{J} \\ 0 \end{bmatrix} \cdot \tau_{ext} \quad (2.9)$$

If the output of the system is angular velocity (we have to convert it from rad/sec to rot/min), we get the output equation as

$$y = \begin{bmatrix} \frac{60}{2\pi} & 0 \end{bmatrix} \cdot \begin{bmatrix} W \\ I \end{bmatrix} (2.10)$$

Finding the transfer function of the system, we get

$$G(s) = \frac{W(s)}{U(s)} = \frac{\frac{K_{add} \times K_t}{JL}}{s^2 + \frac{(JR+dL)}{JL}s + \frac{dR+K_b K_t}{JL}} (2.11)$$

where $W(s)$ is the Laplace form of output signal w and $U(s)$ is the Laplace form of the input signal u and K_{add} is the additional gain value coming from the amplifiers and conversion from rad/sec to rot/min which is given by the,

$$K_{add} = \frac{60 \times 9.6}{2\pi} (2.12)$$

The parameters of the DC motor are given in Table 2.1 (these parameters are taken from [1]).

Table 2.1: DC motor parameters

Parameter	Value
J-moment of inertia	$140 \cdot 10^{-7} \text{ Kg.m}^2$
K_t -torque constant	0.052 Nm/A
K_b -electromotive force constant	0.057 Vs/rad
d-linear approximation of viscous friction	$1 \cdot 10^{-6} \text{ Nms/rad}$
R-resistance	2.5 Ω
L-inductance	2.5 mH

Using Equation 2.9, we can design a SIMULINK model for our system as in Figure 2.4

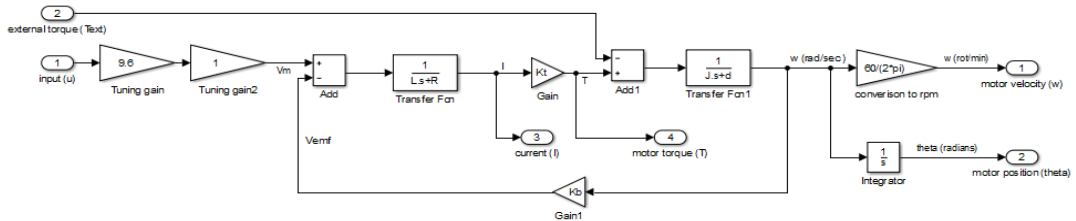


Figure 2.4: DC motor model.

The SIMULINK model in Figure 2.4 can be implemented as a sub-block as in Figure 2.5.

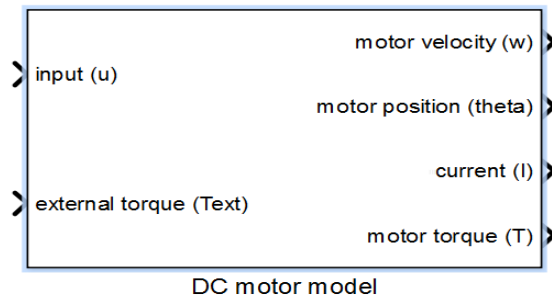


Figure 2.5: The sub-block for the DC motor model

2.3. PID Controller

The main structure of a PID (proportional+ integral+ derivative) controller is

$$C(s) = P + \frac{I}{s} + Ds \quad (2.15)$$

It is widely used in industrial applications. However its parameters should be adjusted intelligently to achieve noble performance in the process control. The controllers have robust structure. The basic configuration of the PID control system is shown in the block diagram in Figure 2.6. The block diagram also gives the notation used for the signals in the control system.

Disturbance noise

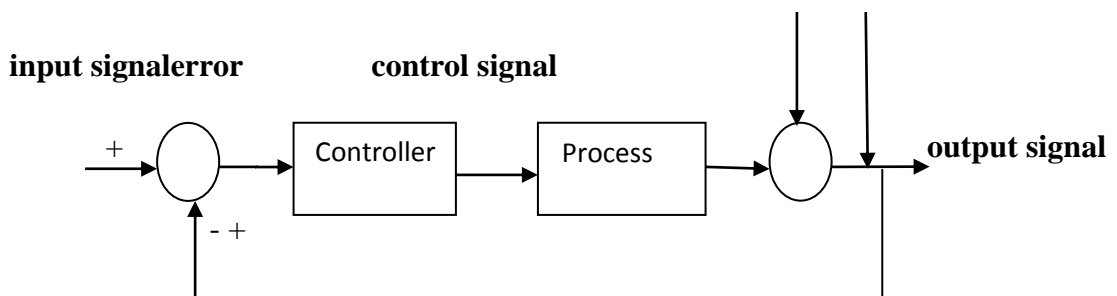


Figure 2.6: General control system scheme.

The implementation of the feedback control scheme in Figure 2.6 in SIMULINK for the DC motor speed control simulations is shown in Figure 2.7.

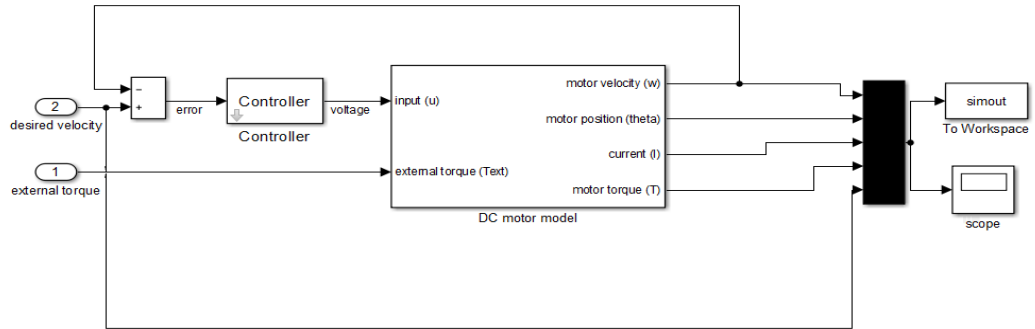


Figure 2.7: SIMULINK control model for DC motor speed control

CHAPTER 3

Simulations

3.1. Simulation Models

In this chapter, the mathematical model of the DC motor system is employed in order to devise controllers for velocity control simulations under different disturbance conditions. The mathematical model gives clues about the possible applicable controller structures. Lucky the system is linear and an extra linearization for the control task is unnecessary. The starting point for the controller design is obtaining the root locus of the open loop system. The transfer function of the open loop system is given by the formula,

$$G(s) = \frac{1.362 \times 10^8}{s^2 + 1000s + 8.476 \times 10^4} \quad (3.1)$$

The transfer function is obtained using Equation 2.11 and Equation 2.12 with the parameters given in Table 2.1

The model is implemented using MATLAB and as the result, we have obtained the root locus plot as in Figure 3.1 for the system.

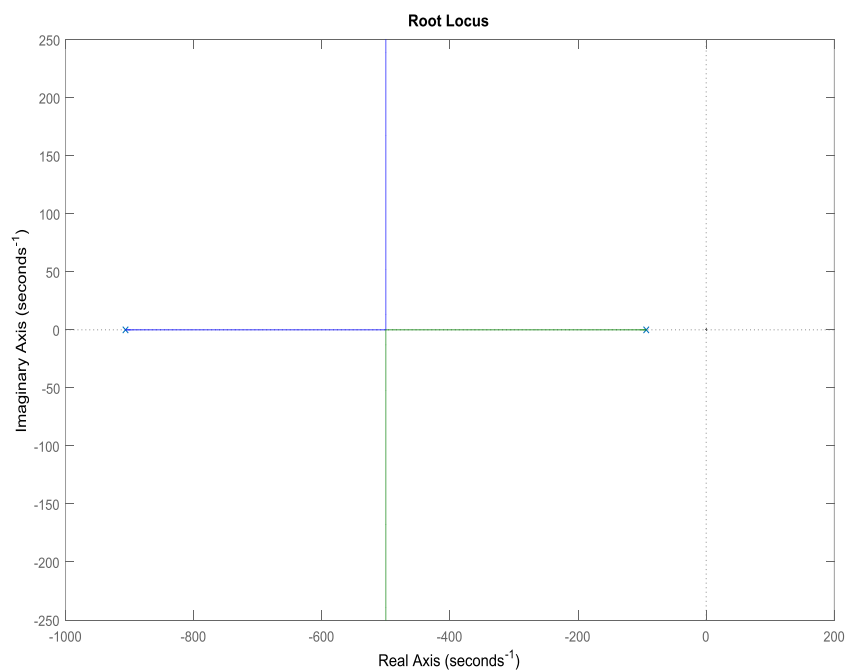


Figure 3.1:Root locus transfer function in Equation 3.1

The root locus of the system can be used to implement different controller structures. As can be observed from the root locus plot the system has originally two poles and no zeros. The poles are both on the left hand side of the imaginary axis and for positive gain values, this system will always be stable. However, the gain value should be chosen wisely to yield comparably the finest performance. The performance can be implemented depending on different criteria such as rise time, settling time, maximum overshoot and steady state error. For us the most important criteria seem to be the steady state error as the system seems to settle down very rapidly. However due to applications of different disturbances the motor may settle down at different velocities rather than the desired velocity values. Therefore, the controller performances will be tested under different disturbance and velocity set point conditions.

3.2 Proportional Control with Root Locus

The first controller structure that is implemented using the root locus method is the simplest one, which is a sole proportional (P) controller. To implement this controller, we moved along the root locus plot in Figure 3.1 and find the point where both poles of the system overlap with each other. These poles coincide at the location -500 and the corresponding gain value is nearly 0.00121. So this gain value is used as the proportional gain value P. Hence the first proposed controller structure is

$$C(s)=0.00121 \quad (3.2)$$

This controller is used in the closed loop feedback system and the performance of the controller is tested under different conditions. In the first simulation, the set point for the reference value of motor velocity is adjusted to 400 rot/min (unit step input with an amplitude of 400) and no disturbance is applied to the system. Under these conditions, the following velocity profile in is observed inFigure 3.2.

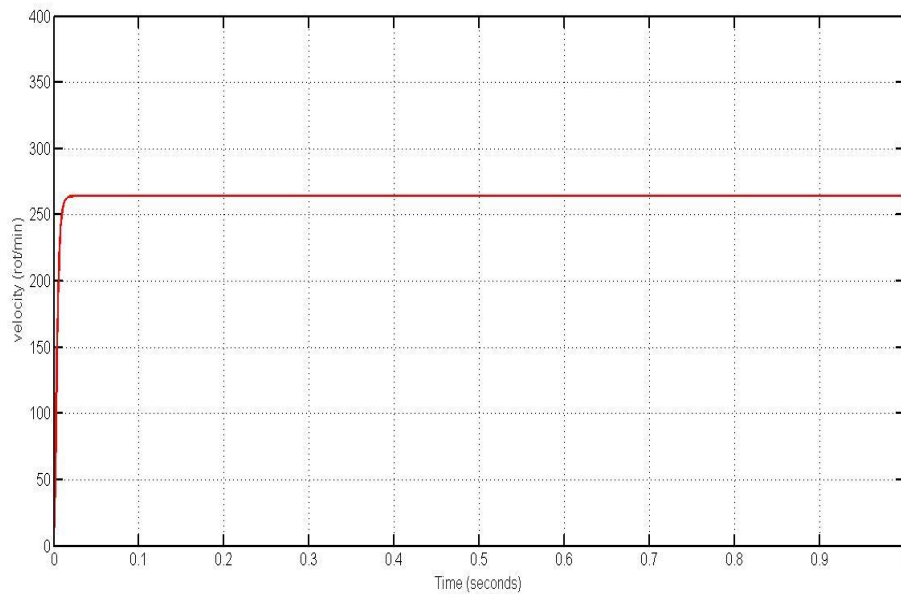


Figure 3.2: Velocity profile obtained using the controller structure in Equation 3.2 for tracking unit step reference signal of 400 rot/min.

From Figure 3.2 it is obvious that there is a very huge steady state error value as expected for P controllers when the proportional gain value is small. Hence, it is necessary to increase the proportional control gain value P but as this happens, it is possible to observe some damped oscillations in the system as well as overshoot. From the root locus plot, when the gain value is taken to be 0.031 the closed loop system poles are moved to locations nearly to $-500 \pm 2010j$. Secondly, we choose a controller with the mathematical structure as

$$C(s)=0.031 \quad (3.3)$$

Corresponding velocity profile obtained this new proportional controller is given in Figure 3.3.

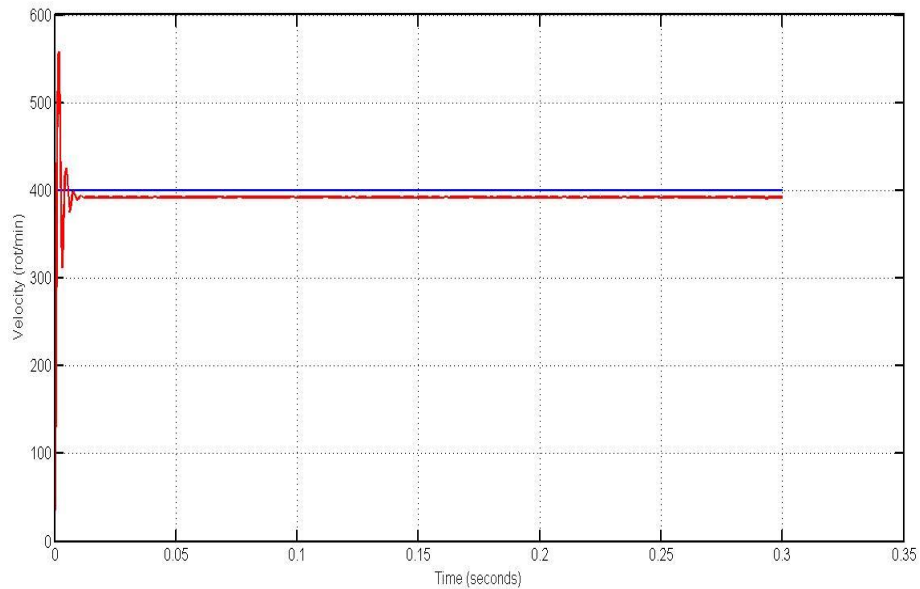


Figure 3.3: Velocity profile (red plot) obtained using the controller structure in Equation 3.3 for tracking unit step signal of 400 rot/min (blue plot).

As seen from Figure 3.3, some under damped oscillations are being observed which are not very outsized in magnitude. However, the output begins to exhibit overshoot, which reaches, nearly to a value of 558 rot/min suddenly after a few milliseconds. The only improvement is observed for the steady state error. The motor velocity settles around 392 rot/min, which is close to the set point of 400 rot/min. It is also intended to monitor the control input (applied voltage to the motor). The corresponding input profile (voltage) applied to the motor changes as in Figure 3.4.

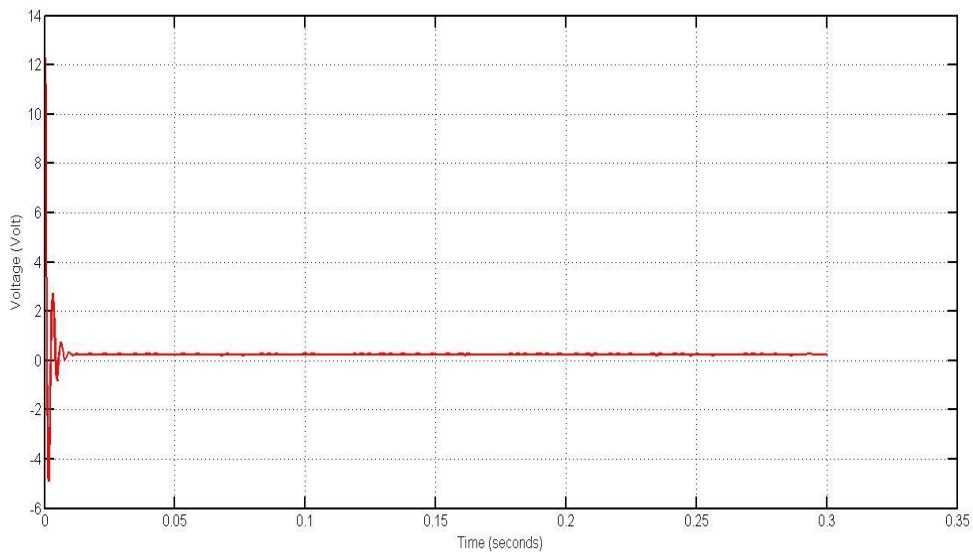


Figure 3.4: Voltage profile when the proportional gain is increased

As observe in the beginning with increased proportional gain value the voltage applied to the motor exceeds 12 volt and -5 volt, which is not a desired situation. If the proportional gain value is further increased, it is sure to observe higher overshoot values and increased damped oscillations. Due to these drawbacks, sole proportional control is not yielding desired performance indices as expected. Hence, new control structures should be tried. Since this controller is not working as satisfactory as desired, no extra disturbance simulations are carried out using this controller.

3.3 Proportional-Integral Control with Root Locus.

In order to observe better steady state performance, it is healthier to offer a PI controller structure that exhibits nearly zero steady state error value for unit step reference change in the set values. However, this time the controller should contain a pole at the origin. The structure of the PI controller is of the form

$$C(s) = P + \frac{I}{s} \quad (3.4)$$

This controller structure can be also written as a gain value P which as applied to as sub-system having a single pole at the origin and a zero at the left hand side of the imaginary as,

$$C(s) = P \times \frac{s + \frac{I}{P}}{s} \quad (3.5)$$

After this step P and I parameters should be determined such that the controller has the desired zero location to eliminate the effect of dominant pole of the original system and necessary gain value to relocate the closed loop system poles. The poles of the original system are located at -906.5804 and -93.4910. Hence, the zero of the controller should be located to -93.4910 to suppress the dominant pole of the original system. This means

$$\frac{I}{P} = 93.4910 \quad (3.6)$$

Having found the ratio of I to P now we can obtain the root locus of multiplication of the original system and the PI controller which gives us the open loop system transfer function T(s) as

$$T(s) = C(s) \times G(s) = P \times \frac{1.362 \times 10^8 s + 1.273 \times 10^{10}}{s^3 + 1000s^2 + 8.476 \times 10^4 s} = P \times G_o(s) \quad (3.7)$$

For T(s), P can be taken as a free gain parameter and adjusting the value of P is very easy by considering the root locus plot of $G_o(s)$ where,

$$G_o(s) = \frac{1.362 \times 10^8 s + 1.273 \times 10^{10}}{s^3 + 1000s^2 + 8.476 \times 10^4 s} \quad (3.8)$$

In Figure 3.5 the root locus plot of $G_o(s)$ is given

\

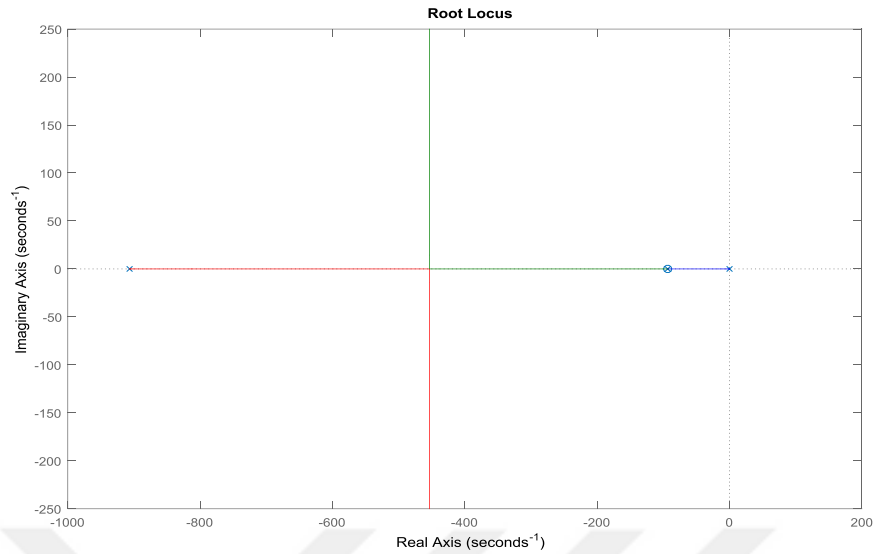


Figure 3.5: Root locus plot of Equation 3.8.

From the root locus plot if the gain value is taken as 0.00151 then the closed loop poles of the system coincides at the location -453 and they do not have any imaginary parts which is assumed to prevent oscillations at the output. Hence, the P parameter should be taken as 0.00151. In this case, using equation 3.6 and taking P as 0.00151, I value can be computed as 0.1412. Hence the controller structure will be

$$C(s) = 0.00151 + \frac{0.1412}{s} \quad (3.9)$$

Using this controller structure, the feedback system was simulated also the corresponding voltage (control signal), velocity, position and current profiles are shown in Figure 3.6.

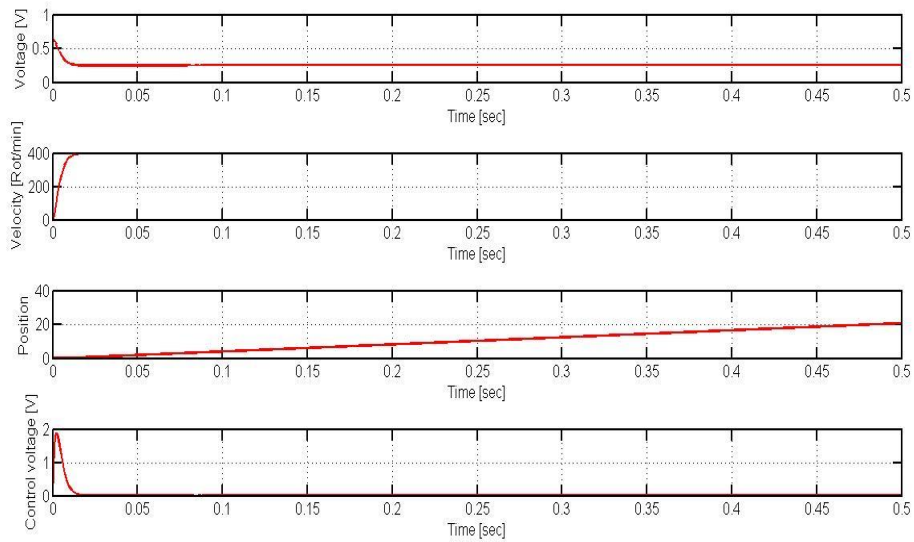


Figure 3.6: Voltage, velocity, position and current profiles for tracking unit step reference signal of 400 rot/min.

As seen from Figure 3.6 the controller works very well for unit step change in reference signal when there are no external disturbances. The steady state error value is zero, there is no overshoot, and undamped oscillations are not observed at the output. The input voltage applied to the motor is not exceeding the limits hence we can declare that the controller works perfectly under no load conditions. Next step is to test the performance of the controller for various load conditions. These loads will act as disturbances. Now, it is required to see the outcome of different disturbances. This time the designed controller test will be connecting with external load and the effect of this load shown in Figure 3.7. The external load is assumed to provide a pulse like external torque of 0.1 Newton-meter between time instances 1 and 2 seconds. The results show that the angular velocity of the motor returns to the reference set value of 400 rot/min very rapidly besides no steady state error is observed. The current and applied voltage values are also in the desired ranges.

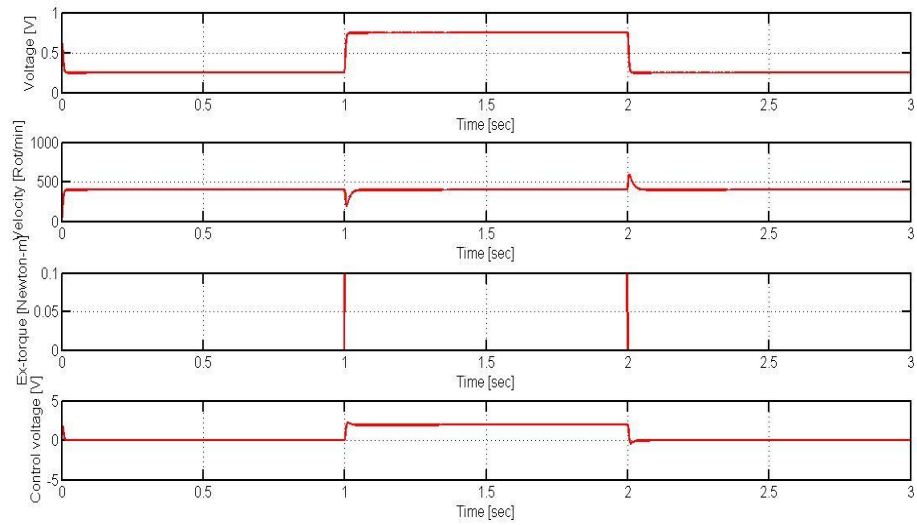


Figure 3.7: Voltage, velocity, external torque and current profiles for unit step reference signal tracking of 400 rot/min in case of pulse type external torque

As an alternative application, we want to apply a reference set point signal for the angular velocity, which is composed of different sinusoidal with some random nature. This signal is given by the formula

$$r(t) = 200 \times \sin(2t) + 150 \times \sin(0.1t) + 400 \times (0.33t) + 1000 \times p(t) \text{ (rot/min)} \quad (3.10)$$

Where $r(t)$ is the reference signal and $p(t)$ is a random signal sampled at every 5 seconds whose mean value is 0 and variance value is 0.02. Thus, this $p(t)$ creates some specific extra jumps at the reference signal. This signal can be in Figure 3.8.

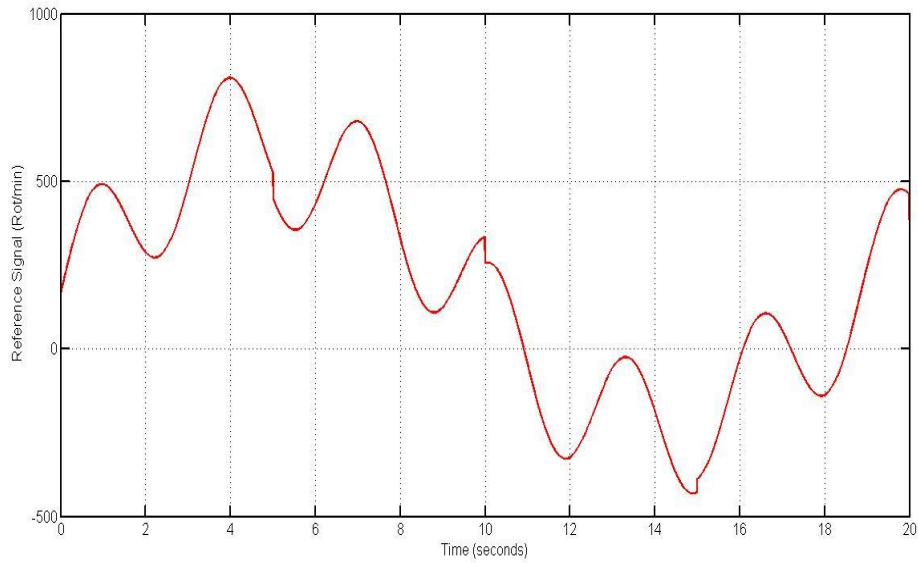


Figure 3.8: Angular velocity(reference signal) given in Equation 3.10

Applying the reference signal in Figure 3.8 coupled with a pulse type external Torque of 0.1 Newton-meter that is applied between the time instances 8th and 10th seconds the controller have achieved the following velocity profile which is plotted with the reference signal together as depicted in Figure 3.9.

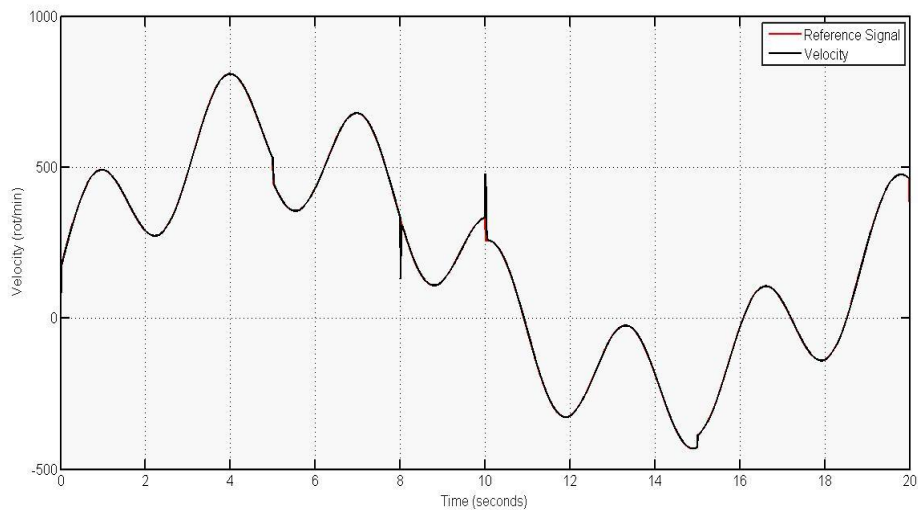


Figure 3.9: Velocity profile when pulse type external torque applied while tracking the reference signal given in Equation 3.10.

In Figure 3.10, the voltage, velocity, external torque and the current profiles are given.

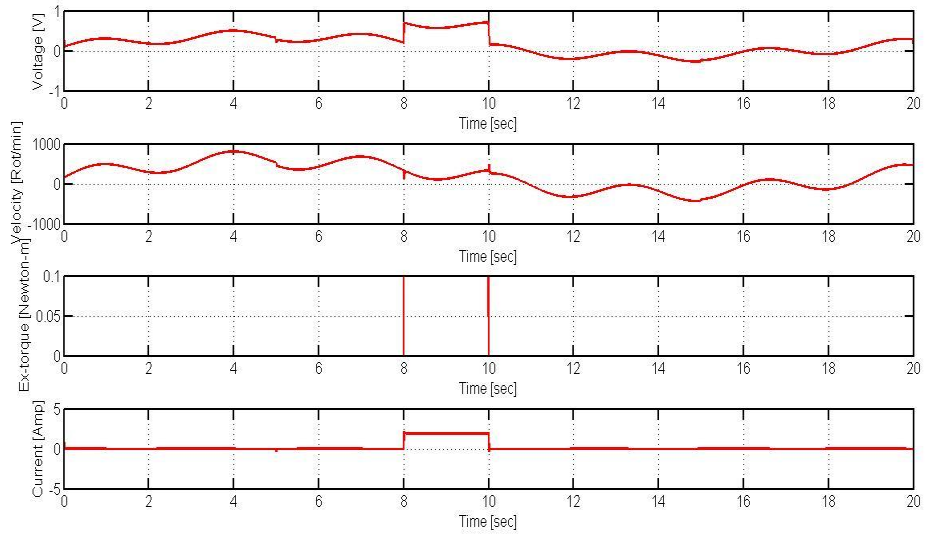


Figure 3.10: Voltage, velocity, torque and current profiles when pulse type external torque applied while tracking the reference signal given in Equation 3.10.

As can be understood from the figures in presence of even sinusoidal reference and pulse like external torques the controller performs very well. As a last simulation, the effect of sinusoidal disturbances coupled with the reference velocity signal given in Equation 3.10 is monitored. The external torque is given by

$$T_{external} = \begin{cases} 0 \text{ Newton - meter, } t \leq 10 \text{ seconds} \\ 0.1 + 0.1 \times \sin(2\pi t) \text{ Newton - meter, } t > 10 \text{ seconds} \end{cases} \quad (3.11)$$

The simulation run for 20 seconds and corresponding voltage, external torque, velocity and current profiles obtained in figure 3.11.

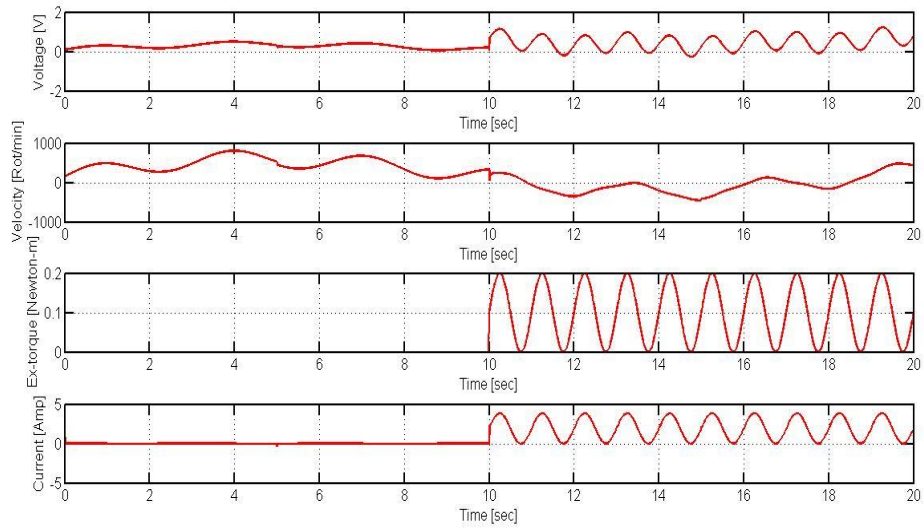


Figure 3.11: Voltage, velocity, external torque and current profiles for sinusoidal reference signal tracking when external torque in Equation 3.11 is applied

In order to see the effect of sinusoidal torque for reference tracking, the reference velocity signal and obtained velocity signal drawn together in Figure 3.12.

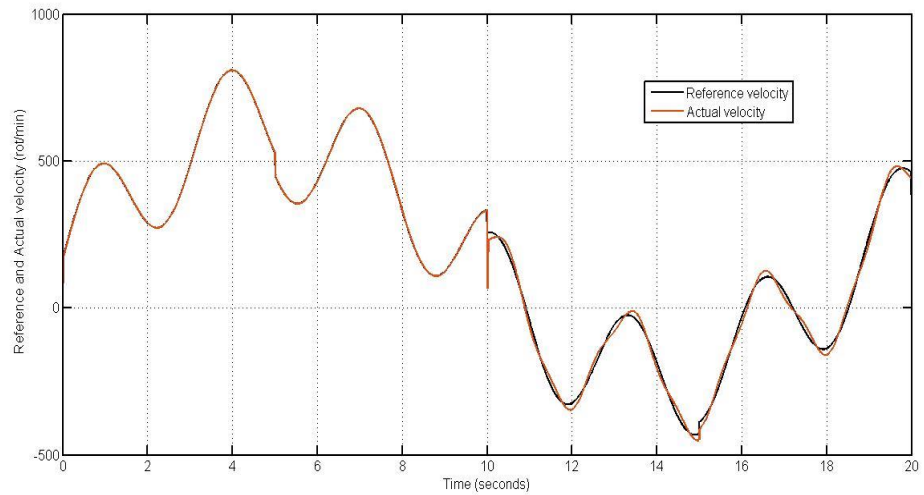


Figure 3.12: Velocity profile for sinusoidal reference signal tracking when external torque in Equation 3.11 is applied

As seen from Figure 3.12, even in case of sinusoidal disturbance the designed controller is able track the reference signal. Additionally, we want to see the effect of increasing the frequency and the amplitude of the disturbance signal. First we increased the frequency of the disturbance signal (the frequency is increased to 2 Hertz) while leaving the amplitude unchanged. Hence, the new external disturbance is taken as

$$T_{external} = \begin{cases} 0 \text{ Newton - meter}, & t \leq 10 \text{ seconds} \\ 0.1 + 0.1 \times \sin(4\pi t) \text{ Newton - meter}, & t > 10 \text{ seconds} \end{cases} \quad (3.12)$$

Obtained actual and reference velocity profiles given in Figure 3.13.

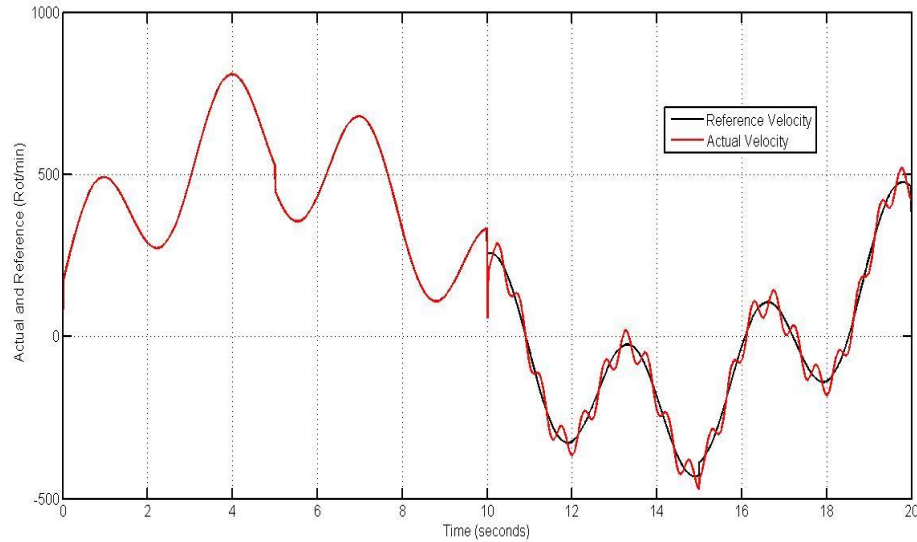


Figure 3.13:Effect of changing the external disturbance as in Equation 3.12 for sinusoidal reference signal tracking

As seen from Figure 3.13, increasing the frequency spoils the tracking performance. Same thing can also be observed for the amplitude change. We also monitored the effect of amplitude change in the disturbance. This time the external disturbance is taken as

$$T_{external} = \begin{cases} 0 \text{ Newton - meter}, & t \leq 10 \text{ seconds} \\ 0.2 + 0.2 \times \sin(2\pi t) \text{ Newton - meter}, & t > 10 \text{ seconds} \end{cases} \quad (3.13)$$

Where the frequency of the sinusoidal term is 1 Hertz however, the amplitude is 0.2.

The reference and the actual velocity profiles are shown in Figure 3.14.

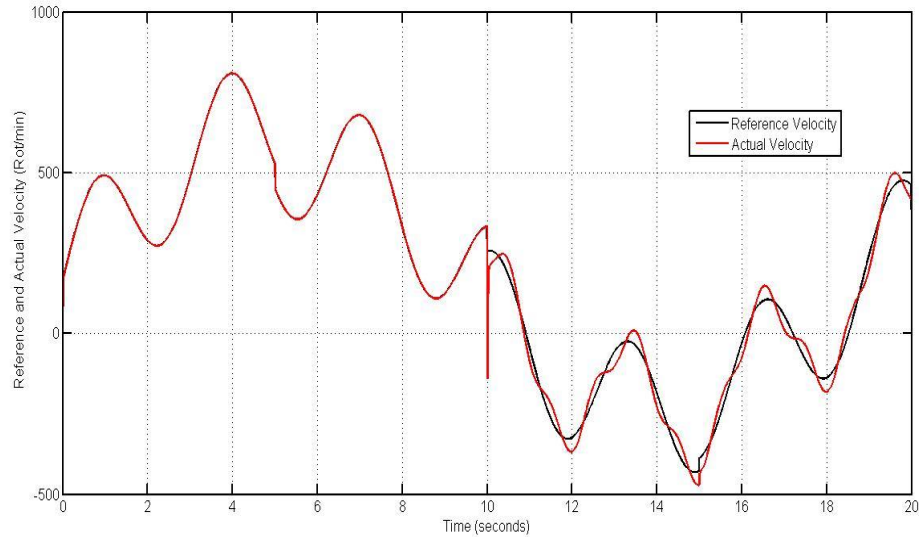


Figure 3.14:Effect of changing the external disturbance as in Equation 3.13 for sinusoidal reference signal tracking.

As seen from figure 3.14 increasing the amplitude of disturbance also spoils the performance of the controller for reference signal tracking task. As a last simulation, the effect of increasing the reference signal frequency is monitored in case of pulse disturbance. This time the reference signal is taken as

$$r(t)=200\times\sin(20t)+150\times\sin(0.1t)+400\times(0.33t)+1000\times p(t) \text{ (rot/min)} \quad (3.14)$$

where $r(t)$ also includes a high frequency sinusoidal wave component whose angular frequency is 20 rad/sec. Besides, in the simulation we also imposed the system with a pulse like external torque disturbance of 0.1 Newton-meter that is applied between 8th and 10th second. The voltage, current, velocity and external torque profiles obtained in Figure 3.15.

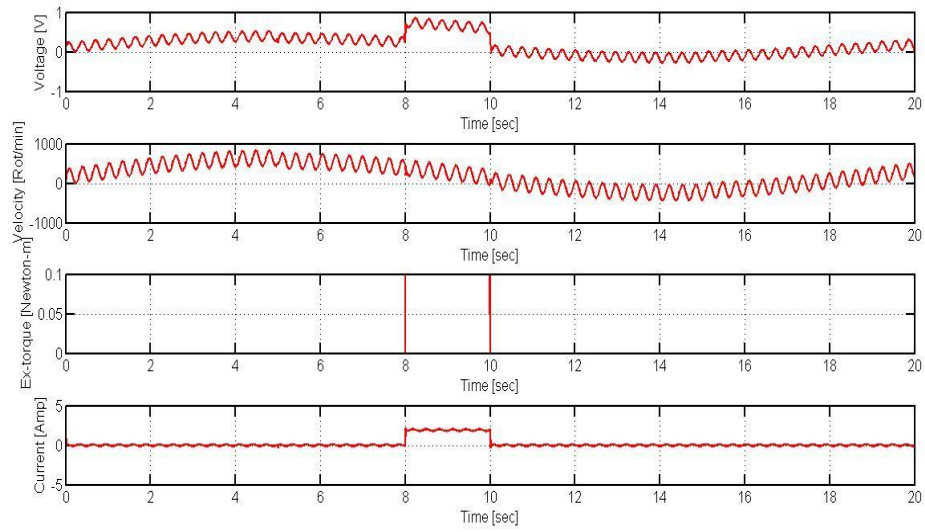


Figure 3.15: Voltage, velocity, external torque and current profiles in case of external square torque

To see the effect in reference signal tracking, both the reference velocity signal and the actual velocity signal are drawn together in Figure 3.16.

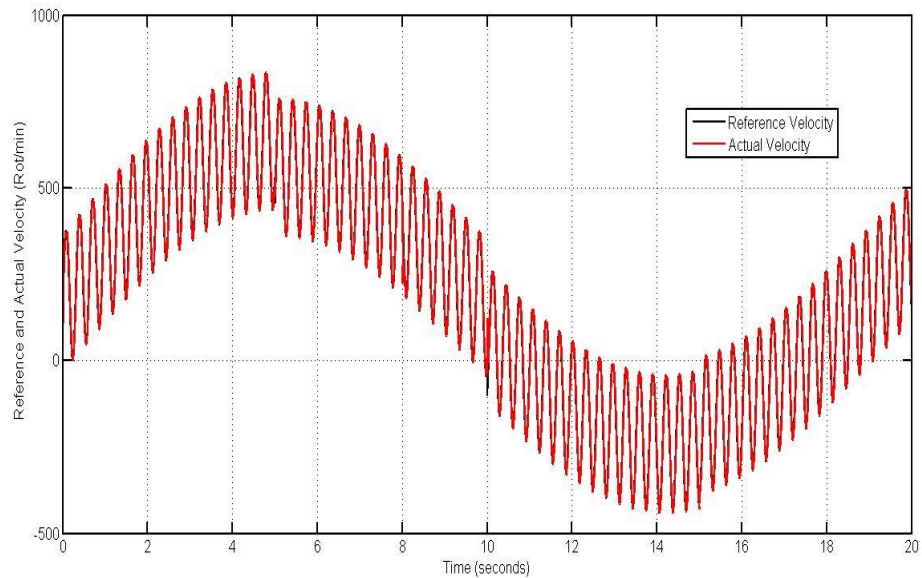


Figure 3.16: Reference and actual velocity profile in case of external square torque.

It seems the velocity-tracking task accomplished well. However, to have a better insight, Figure 3.16 drawn with higher resolution between the 7th and 11thseconds in Figure 3.17 to observe the effects of disturbance between 8th and 10th seconds.

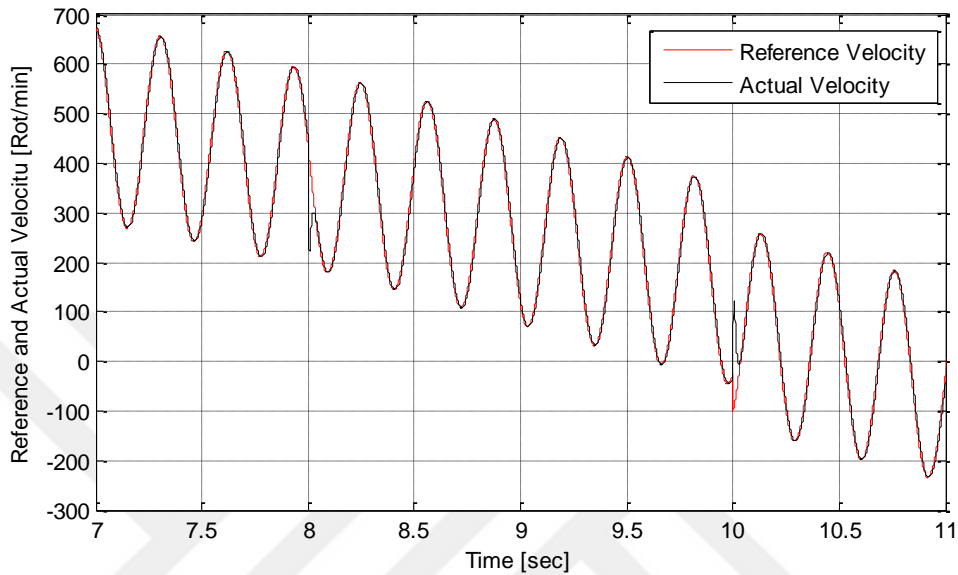


Figure 3.17: Reference and actual velocity profile with higher resolution in case of external square torque.

As seen from Figure 3.17 the tracking task is nearly perfect except for the time instances that the disturbance pulse is applied. Even few milliseconds after those instances the motor begins to track the reference velocity signal very rapidly by the influence of the controller.

CHAPTER 4

Real Time Applications

4.1 Methodology

The designed controller in Chapter 3 is tested for real time applications in this section. Due to the nature of the real time application, some unexpected outputs might be observed and the controller structures obtained in the simulation models might turn out to be ineffective. This drawback is also observed in the real time application we conducted. Hence, an extra system identification step coupled with the controller design is performed in this chapter for real time controller design.

4.2. Test of the Developed Simulation Model Controller in Real Time Application

The first application is utilizing the controller given in Equation 3.9 and checking its performance in real time application. This controller accomplishes many different velocity-tracking tasks successfully under different disturbance conditions in simulations. Hence, it is a good candidate to start with. This time a real time application model for the DC motor velocity control experiment is implemented and the controller in Equation 3.9 is set as the PID controller structure. The real time SIMULINK model is shown in Figure 4.1.

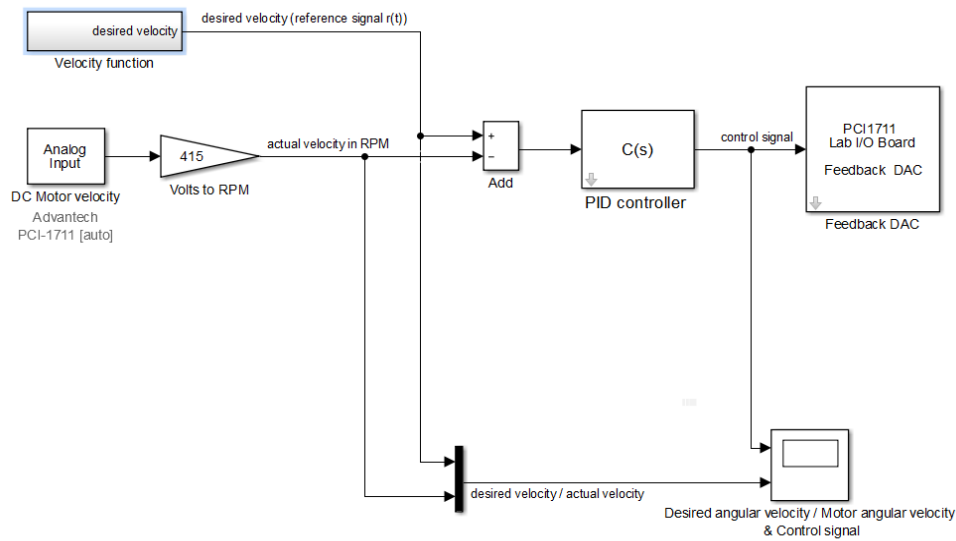


Figure 4.1: The real time SIMULINK model

In this model, the analog voltage signal attained from the Analog Input block is multiplied by 415 to convert it to the rotation per minute (rot/min) value. This signal gives us the actual velocity in rot/min. This function is compared with the desired velocity signal. The desired velocity signal (reference signal) is given by the formula,

$$r(t) = 200 \times \sin(2t) + 150 \times \sin(0.1t) + 400 \times (0.33t) + 1000 \times p(t) + 1000 \times s(t) \text{ (rot/min)} \quad (4.1)$$

In Equation 4.1, $p(t)$ is a random signal which is sampled at every 5 second with a variance value of 0.02 and a mean value of 0 and $s(t)$ is a square wave with 0.3 amplitude and 0.1 Hertz frequency. As seen from the block diagram in Figure 4.1, the difference between the desired velocity and actual velocity signal is inserted into the PID controller given in Equation 3.9 and the corresponding control signal is obtained. The control signal is fed to the Feedback DAC and it is supplied to the system and the system is run by this control signal finally. The obtained desired velocity and actual velocity signals and the fed control signal to the real time system are given in Figure 4.2.

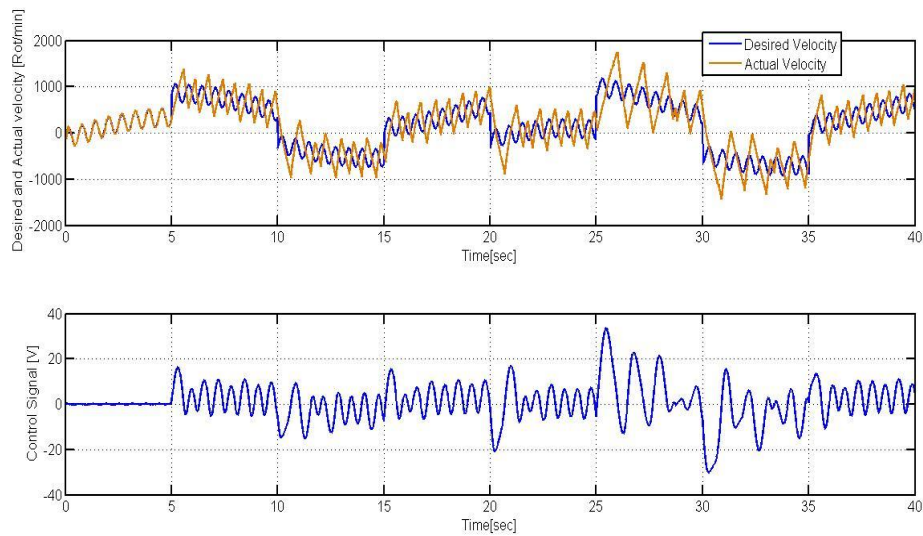


Figure 4.2:Desired, actual velocity and voltage signals for real time system using the controller given in Equation 3.9.

As can be understood from Figure 4.2, the best control strategy obtained in the simulation models in Chapter 3 is insufficient to make the system track the desired velocity signal. Hence, a system identification phase should be implemented beforehand and a new controller structure should be proposed according to the results of the system identification phase.

4.3. System Identification

System identification is the process of obtaining an approximate model of the considered system based on the input and output data. If the system to be identified is known to be stable and further assumed to be linear this mission is straightforward. Luckily, the DC motor control system seems to possess these two characteristics. To obtain the approximate model structure, first the system is driven by a specific control signal and then based on this control signal the system output (for our case the output is the motor angular velocity) is recorded. Finally the input and output signals are used altogether to identify the system structure.

4.3.1. System Identification with Sinusoidal and Random Signal

For this purpose real time model structure in Figure 4.3 is used.

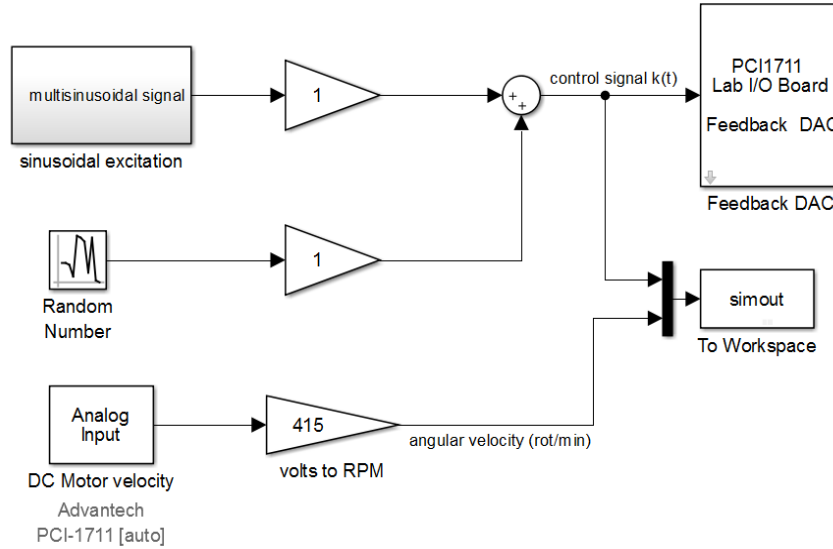


Figure 4.3:Real time model structure

In the model in Figure 4.3, the control signal is obtained as the summation of some sinusoidal signals coupled with a random function, which is given by the formula,

$$k(t)=0.2 \times \sin(t)+0.4 \times \sin(0.2t)+0.4 \times (6.7t+0.3)+0.2 \times \sin(10t)+p(t) \text{ Volt} \quad (4.2)$$

where $p(t)$ is a random signal with Gaussian distribution with 0.02, variance and 0 mean value that sampled at every 0.1 seconds. Using this control signal (input data), the corresponding angular velocity signal (output data) is obtained in real time application and these values are recorded. After this step, the input and output data are used in the identification toolbox of MATLAB to obtain the approximate identified model. System identification toolbox has many facilities. One can obtain the approximate transfer function for the system as well as the state space model by using system identification toolbox. Our intention is to obtain the transfer function. As the ideal system model has two poles and no zeros we decided to use the same

transfer function structure and run the system identification toolbox accordingly. The transfer function obtained as the result of system identification step is

$$G(s) = \frac{2.55 \times 10^6}{s^2 + 505.5s + 840.8} \quad (4.3)$$

This transfer function has poles at the locations -503.8082 and -1.6689 (dominant pole). The corresponding root locus plot for the transfer function at Equation 4.3 is shown in Figure 4.4.

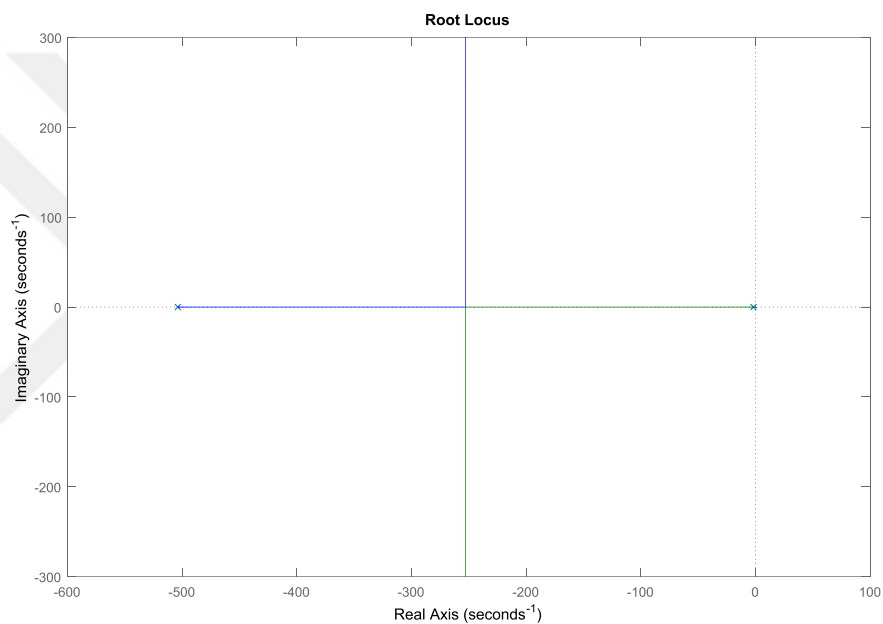


Figure 4.4:Root locus plot for the transfer function in Equation 4.3

As seen the transfer function obtained due to system identification step in Equation 4.3 is very different form the transfer function given in Equation 3.1 corresponding to the mathematical model.

4.4 Design Update and Test of Controller for the Identified Real Time System

Having the root locus plot of the identified system, it is possible to implement new controllers to control the identified system instead of the simulated system. Hence, a similar strategy is applied as done in Chapter 3 to design the controller for the identified system. We proposed a PI controller,

$$C(s) = P + \frac{I}{s} \quad (4.4)$$

That has pole at the origin and a zero at the location of the dominant pole of the identified system (the controller will have a zero at the location -1.6689). Hence, the controller can be restructured as

$$C(s) = P \times \frac{s + \frac{I}{P}}{s} \quad (4.5)$$

Where

$$\frac{I}{P} = 1.6689 \quad (4.6)$$

Having found the ratio of I to P, now we can obtain the open loop system transfer function $T(s)$ which is multiplication of the identified system and the PI controller,

$$T(s) = C(s) \times G(s) = P \times \frac{2.55 \times 10^6 s + 4.256 \times 10^6}{s^3 + 505.5 s^2 + 840.8 s} = P \times G_o(s) \quad (4.7)$$

Indeed, there is a pole-zero cancellation in $T(s)$ since zero of the controller is taken the same as the pole of the identified system. Thus the minimal realization of $T(s)$ (after pole-zero cancellation) is

$$T(s) = P \times \frac{2.55 \times 10^6}{s^2 + 503.8082 s} \quad (4.8)$$

There is now only a single parameter P left to complete the design and for this purpose, we obtain the root-locus of $G_o(s)$ in Figure 4.5.

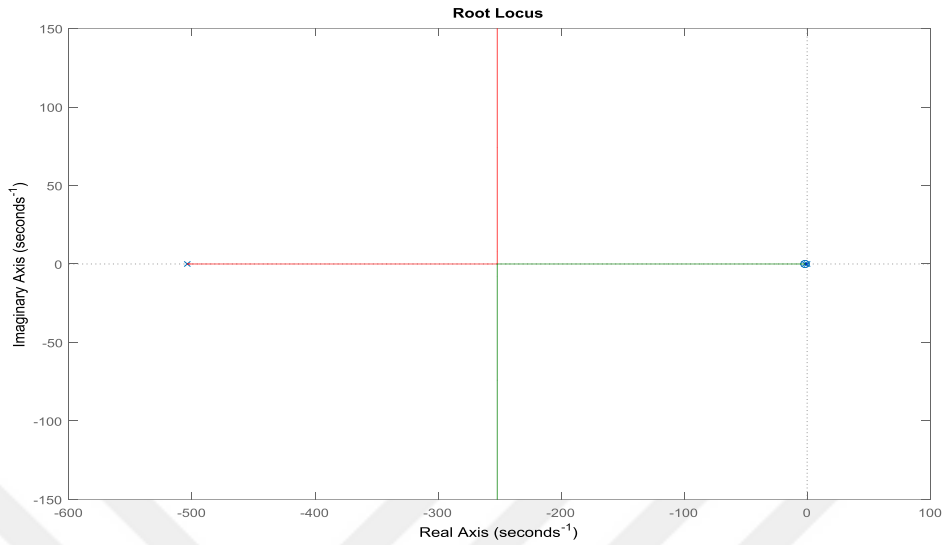


Figure 4.5:Root locus plot for Equation 4.8

From the root locus plot if the gain value is taken as 0.0249 then the closed loop poles of the system coincide at the location -252 and they do not have any imaginary parts which is assumed to prevent undamped oscillations at the output. Hence, the P parameter should be taken as 0.0249. In this case, controller structure will be

$$C(s) = 0.0249 + \frac{0.04155}{s} \quad (4.9)$$

We put this controller structure as the PID controller block shown in Figure 4.1 and the real time application run for the reference signal $r(t)$ given in Equation 4.1. The resultant angular velocity and desired velocity signal profiles with the controller output values as a function of time are shown in Figure 4.6

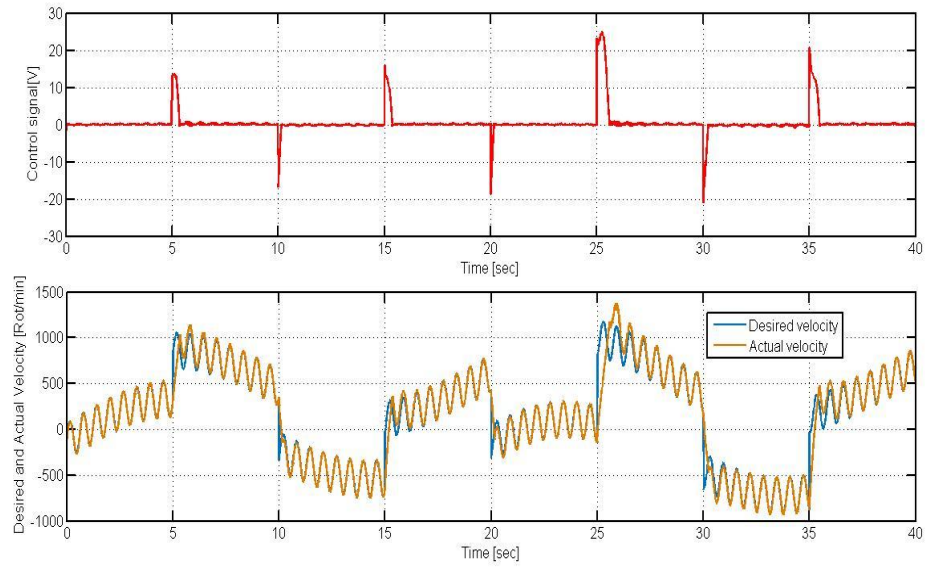


Figure 4.6: Voltage and velocity profiles for sinusoidal reference signal tracking using controller in Equation 4.9

We also tested the performance of the controller for square wave velocity tracking. Hence, the reference signal is given as

$$r(t)=1000 \times s(t) \text{ (rot/min)} \quad (4.10)$$

Where $s(t)$ is a square wave of 0.3 amplitude, and 0.1 Hertz frequency. Using the same controller with this new reference signal, we observed the following control signal and velocity profiles shown in Figure 4.7.

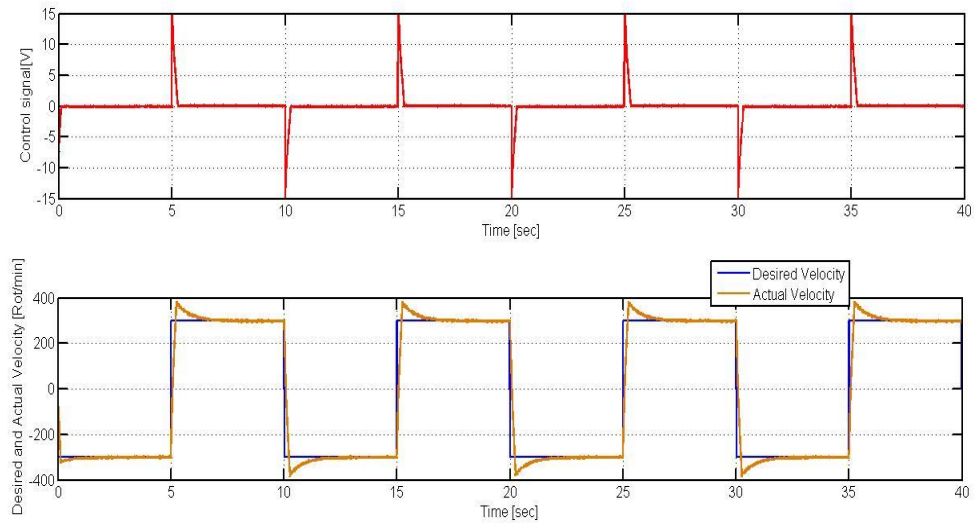


Figure 4.7: Voltage and velocity profiles for square reference signal tracking using controller in Equation 4.9.

As seen from the Figures 4.6 and 4.7, the controller performs comparably well. However, at times when there are sudden changes (due to jumps originating from square waves or sudden jumps observed due to application of random signals in sinusoidal waveform) it takes some time for the controller to track the reference signal. Besides some overshoot is observed especially while tracking the square wave in Figure 4.7. To eliminate overshoot, the first alternative is further update of the controller parameters around their selected values. This is possible by decreasing the amount of integral given to the system. However, decreasing the integral may also decrease the steady state performance and the response may reach to steady state value more slowly. To eliminate this side-affect, this time the proportional gain should be increased slightly. Nevertheless, it should be considered that these parameters changes should be around the selected parameters that are given on the controller structure in Equation 4.9. The second alternative is to change the identification parameters or to reapply the identification process due to some different input signal. We will choose the first alternative. For this reason, we have run the real time application for velocity tracking of square wave reference signal given in Equation 4.10 by decreasing the value of integral according to the parameter

set given in Table 4.1. To see the effect of decreasing the integral we calculated the overshoot and the steady state error of the system by the formulas

$$\text{overshoot}(\%) = 100 \times \frac{v_{max} - v_{ss}}{v_{ss}} \quad (4.11),$$

$$e_{ss} = v_{ref} - v_{ss} \quad (4.12),$$

In Equations 4.11 and 4.12 v_{max} is the maximum value of the angular velocity observed in the real-time application v_{ss} is the steady state value of the angular velocity signal and v_{ref} is the reference signal amplitude for the square wave which is 300 rot/min. We also want to see the rise time values t_r which is the first time instance the response passes the steady state value. The results for these performance indices are also tabulated at Table 4.1.

Table 4.1: Motor velocity, overshoot, steady state error and rise time values

Parameters	Observations				
	v_{max} (rot/min)	v_{ss} (rot/min)	Overshoot (%)	e_{ss}	t_r (sec)
P=0.0249, I=0.04155	387	300	29	0	0.1095
P=0.0249, I=0.02	340	300	13	0	0.1174
P=0.0249, I=0.01	320	300	6	0	0.111
P=0.0249, I=0.005	310	300	3	0	0.105
P=0.0249, I=0.002	306	300	2	0	0.111
P=0.0249, I=0.001	304	300	1	0	0.108
P=0.0249, I=0	302	298	0	2	0.107

As observed from Table 4.1, the most satisfactory results are obtained when there is very small integral I=0.001. When I=0, we began to observe some steady state error in the system. Thus we update the I parameter to I=0.001 and the corresponding velocity and control signal profiles are obtained as in Figure 4.8 for the reference signal given in equation 4.10.

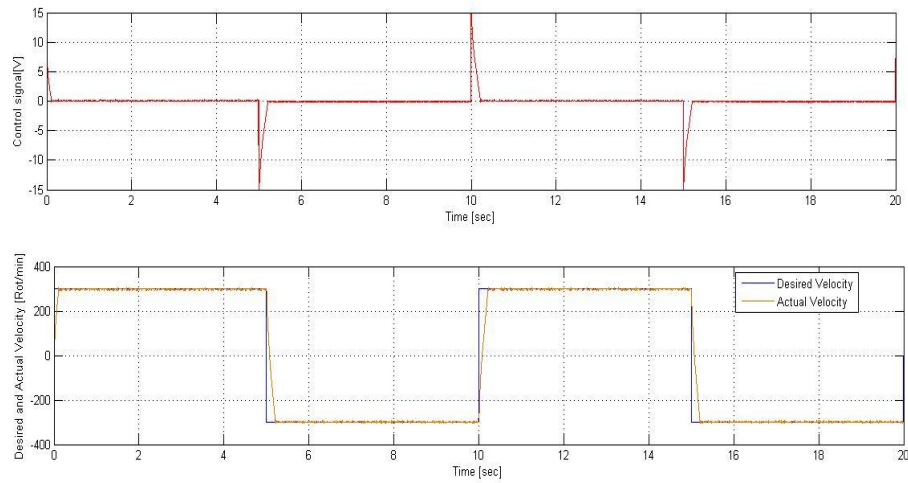


Figure 4.8: Voltage and velocity profiles when $P=0.0249$ and $I=0.001$ for square reference signal tracking

We also want to see the performance of the updated controller for sinusoidal reference signal tracking. Hence the updated controller with $P=0.0249$ and $I=0.001$ is also check in case of a reference signal given in Equation 4.1. The results are given in Figure 4.9.

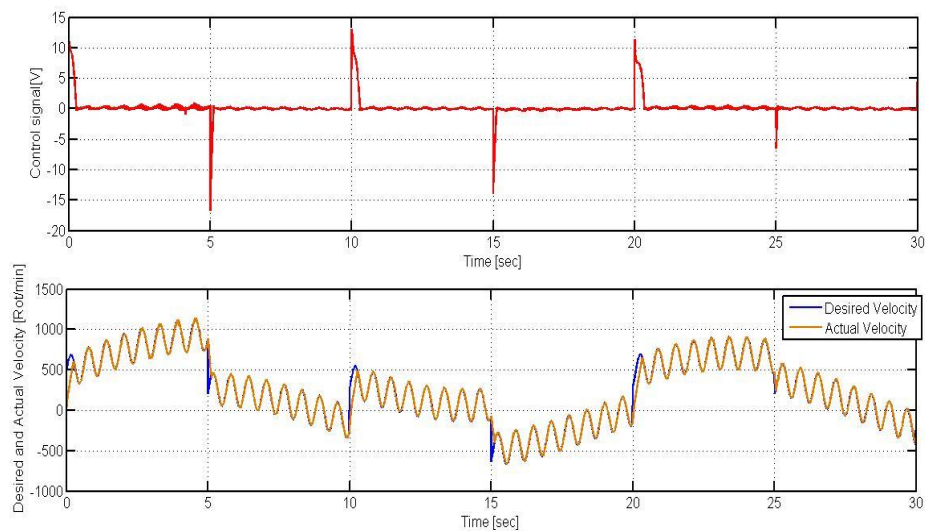


Figure 4.9: Voltage and velocity profiles when $P=0.0249$ and $I=0.001$ for sinusoidal reference signal tracking

As can be seen from the results, the controller is very successful for reference signal tracking. Only one small extra additional change can be inserted into the controller structure. That is a saturation block that limits the output (higher limit is 2.5 Volt and lower limit is -2.5 Volt) of the controller to prevent outputs with high amplitudes as in Figure 4.10.

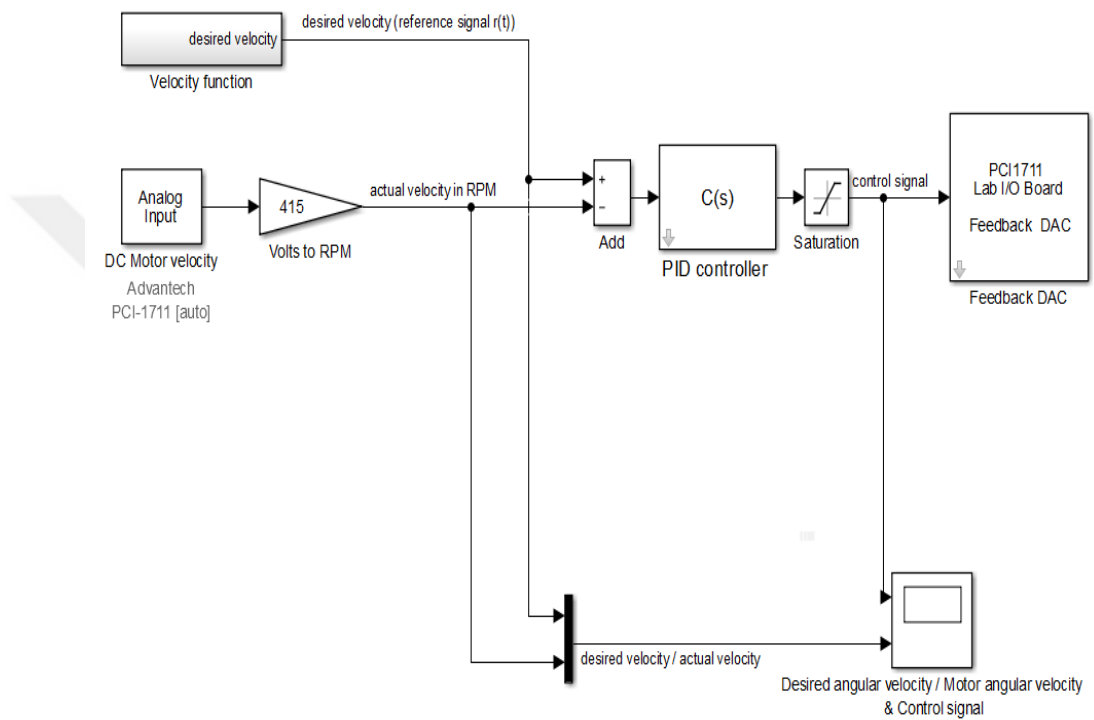


Figure 4.10: The real time SIMULINK model with a saturation device (block)

This new design with saturation block tested by using the reference given in Equation 4.1 and the results given in Figure 4.11

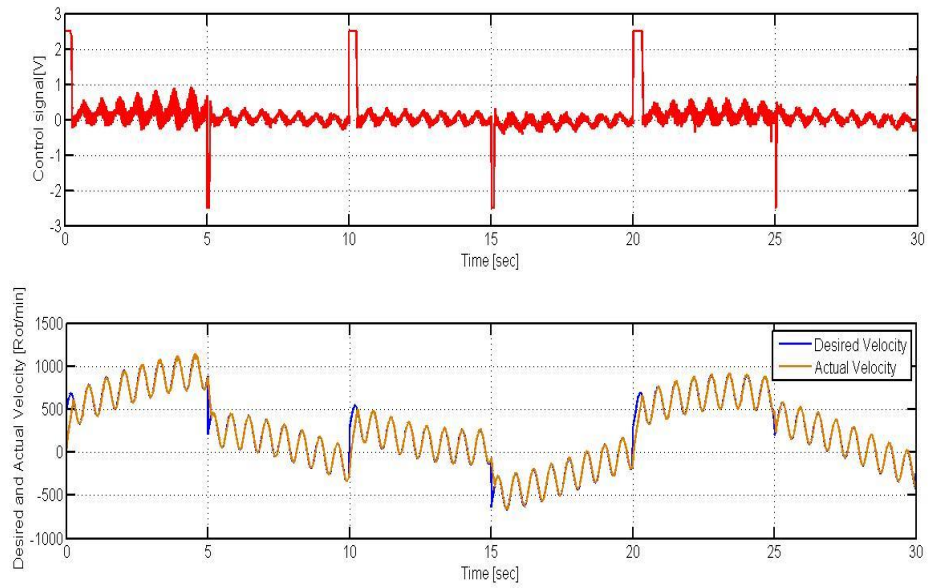


Figure 4.11: Voltage and velocity profiles with the effect of saturation block for sinusoidal reference signal tracking

We also want to see the effect of using solely square wave reference signal as given in Equation 4.10. The results are shown in Figure 4.12.

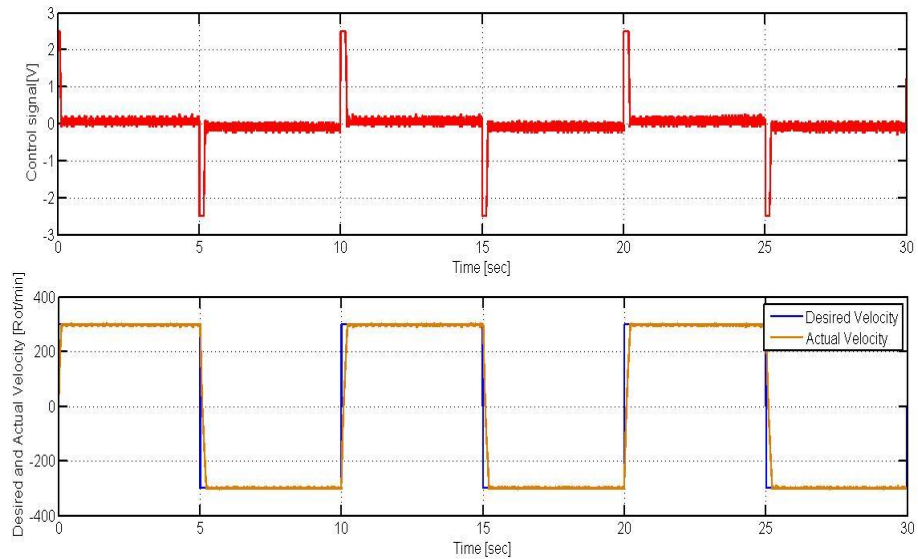


Figure 4.12: Voltage and velocity profiles with the effect of saturation block for square signal reference tracking

Applying the saturation block the control signal is limited. Nevertheless, this new design did not cause any drastic alteration in velocity tracking performance of the controller. Thus, the controller now can be challenged by a new complication: its performance can be tested in applications including some external disturbance. The external disturbance for this system can be given by a kind of magnet. The magnet has two positions one is when it is not touching the moving disc of the DC motor (no load condition) and the other one is the case when it is touching to the disc (full load condition). Unfortunately, there are no other easy means or extra devices in the experimental set-up to apply as a source of disturbance in real time application that applied to test the controllers' performance. Therefore, the disturbance will be on or off type. First, we tested our system with a reference signal of

$$r(t)=1000\times s(t) \text{ (rot/min)} \quad (4.13)$$

Where $s(t)$ is a square wave with 1 amplitude and 0.1 Hertz frequency. The magnetic disturbance is lowered at the 10th second and it is removed nearly at 40th second. The following results in Figure 4.13 are obtained.

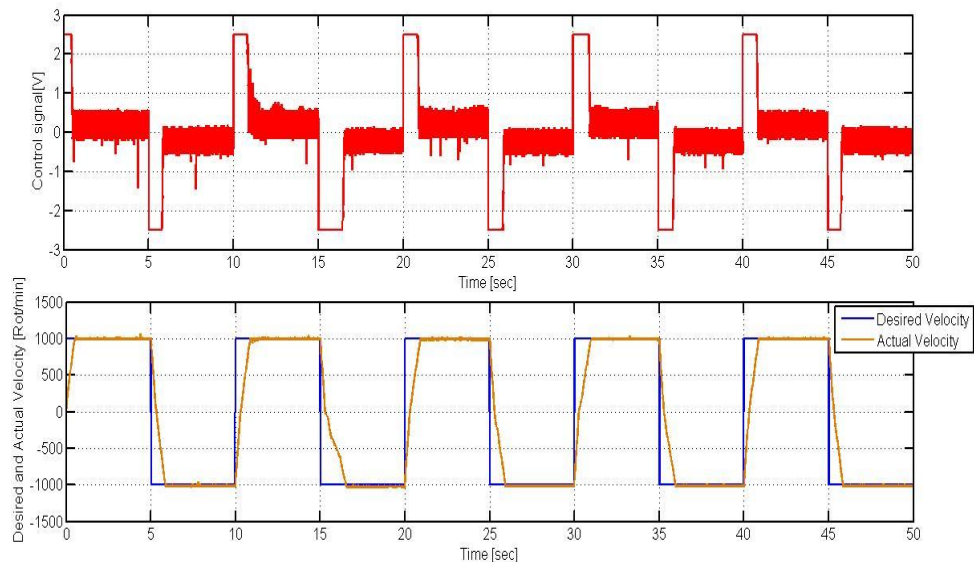


Figure 4.13: Voltage and velocity profiles with the effect of magnetic disturbance for square reference signal tracking

From Figure 4.13, it can be realized that between the time instances 10 to 15 the controller produced excessive voltage signal to catch the reference velocity value of 1000 rot/min. Between the time instance 15 to 20 seconds the reference signal is suddenly changes from 1000 to -1000 rot /min and this causes longer duration for the system to settle down at the steady state value of -1000. However, in the proceeding signal cycles, the system adapts itself to the disturbance change and it becomes easier for the controller to follow the reference signal. As a last example, we want to test the performance of the controller when some sinusoidal are used as the reference signal. Hence, the equation 4.1 is used as the reference signal and the disturbance is applied at the 10th second of the simulation while it is removed ant the 30th second. The results are shown in Figure 4.14.

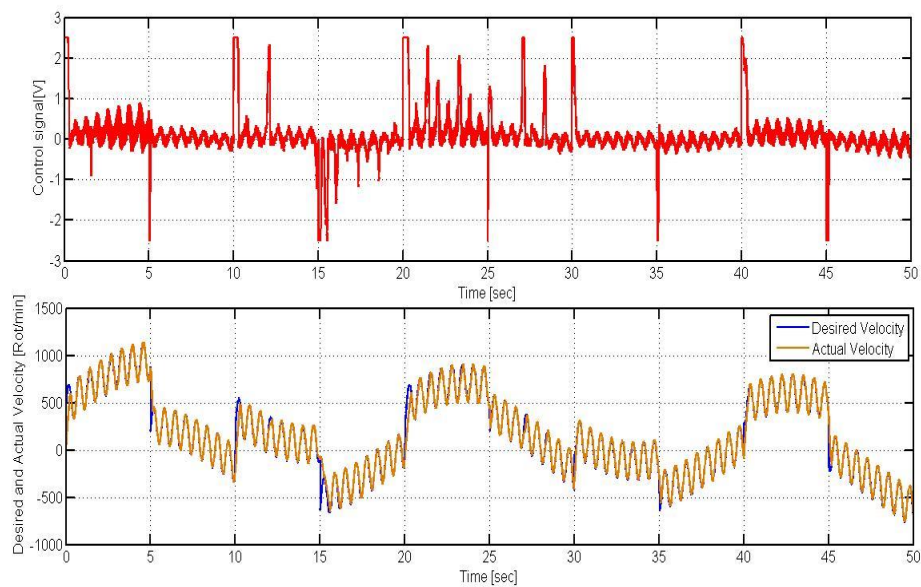


Figure 4.14: Voltage and velocity profiles with the effect of magnetic disturbance for sinusoidal reference signal tracking

As seen from the Figure 4.14 at instants where the disturbance is more effective, excessive voltage supplied by the controller to the system, nevertheless, the controller is successful and the reference signal tracked easily.

4.5 Controller Design with P Controller

One thing that strikes to the eyes of a careful observer for the controller design is that using the initial controller parameters $P=0.0249$ and $I= 0.04155$ is not as good choice to improve the performance criteria. Instead we obtained better results with the controller parameters $P=0.0249$ and $I= 0.001$. What is the reason to decrease the ‘I’ value so much to have the best performance? The answer for this question lies in the root locus plot given Figure 4.4 and the Equation 4.3 that gives the transfer function of the identified system. This transfer function has poles at the locations -503.8082 and -1.6689 (dominant pole). As one can quickly realize one of the poles of the identified open loop system is very close to zero (-1.6689). This situation creates a very important benefit to minimize steady state error value. We will check two different cases. The first case is the case when $P=0.0249$ and $I=0$ and the second one is the case when $P=0.0249$ and $I=0.001$ and see the effect of these two controller parameters mathematically in computation of the steady state error value,

The steady state error value of a linear system is computed by the formula,

$$e_{ss} = \lim_{s \rightarrow 0} sE(s) = \lim_{s \rightarrow 0} s \frac{R(s)}{1+G(s)C(s)} \quad (4.14)$$

In Equation 4.14, e_{ss} is the steady state error value in time domain, $E(s)$ is the Laplace domain error signal, $R(s)$ is the Laplace domain reference signal, $G(s)$ is the system transfer function and $C(s)$ is the controller transfer function. Let us take the reference signal as unit step function whose magnitude is 300. In this case

$$R(s) = \frac{300}{s} \quad (4.15)$$

Using Equation 4.15 in Equation 4.14 the steady state error for unit step reference of 300 will be

$$e_{ss} = \lim_{s \rightarrow 0} sE(s) = \lim_{s \rightarrow 0} \frac{300}{1+G(s)C(s)} \quad (4.16)$$

Let us use the controller parameters $P=0.0249$ and $I=0.001$ (PI controller) and use the identified system structure given in Equation 4.3 as the $G(s)$. In this case, e_{ss} will be equal to 0. This is because of the identified system is a type-0 system (no poles at the

origin) and this system is controlled by a controller which has a single pole at the origin (PI controller always have a pole at the origin). Now, let us use the control parameters $P=0.0249$ and $I=0$ (solely P controller) and use the identified system structure given in Equation 4.3 as the $G(s)$, in this case e_{ss} will be equal to 3.93 (namely 3.93 rot/min error in case of a unit step reference change of 300 rot/min). The reason of non-zero steady state error is that 0-type system $G(s)$ is being controlled by a controller which does not contain any poles, that will sure to bring a non-zero steady state error to the system. However, the dominant pole of the system is so close to the origin such that it nearly plays the role of a pole at the origin and hence the steady state error value is limited even if the proportional gain value P is not increased too much. For this reason, if only P controller is used instead of PI controller, the change in the steady state value is not very significant. Hence, to control the system a very slight integral control is enough. As checking the root locus plot of the identified system given in 4.4 same deductions can be obtained from another perspective by only designing a P controller. If we want to design solely a P controller for the identified system the best P value should be $P= 0.0247$. This value is the gain value where the two poles of the root locus plot collide with each other. As seen, this P value is very close to the P value selected for the actual controller ($P=0.0249$ for the designed controller). Thus choosing $P=0.0249$ and taking I as small as possible to reset the steady state error and prevent overshoot is a perfect idea for the DC motor speed control system.

CONCLUSION

In this thesis simulative and real time DC motor speed control is addressed. Many different methods can be applied for this purpose. One of the most convenient methods is to use a PID controller. This thesis tries to give a simple idea about how to determine and later adjust the parameters of the controller both in simulation and real time application. The DC motor system is generally assumed to be linear system and besides the order of the system is just second order. For these reason, designing a controller might seem straightforward for a simulation. However, in real time application this process is much more difficult. For simulation, the controller parameters are determined using root locus method. However, it is also observed that the controller parameters obtained for the simulation are proven unsuccessful in the real time application. This problem might arise due to imperfections in the linear model of the system and the uncertainties in the motor parameters. Besides, there is always some non-linearity inherent due to nature of the real time application. Hence, in order to develop competent controllers, the linear mathematical model revised and the non-linearity of the system should consider in the mathematical equations of the system. For the controller design task in real time application, instead of obtaining the exact mathematical model of the system, it is required to obtain a new approximate model (again second order) that can be employed instead of the main model with the preliminary parameter settings. To obtain this approximate model a system identification application is carried out and a second order approximate model of the real time system is obtained. After this approximate model is obtained, through using root locus method again, a new controller is designed for the real time system. This new controller is tested in the real time applications and by a few parameter changes, it becomes more successful. The structure of the controllers obtained for both simulation and real time application are either P or PI controller type. It is observed that P or PI controllers with appropriately adjusted parameters could be sufficient to nearly accomplish most of the control tasks such as reference signal tracking, and enduring to external disturbances. With the use of these designed controllers, there are also improvements nearly in all of the performance indices. For the future work, we want to put machine learning methods and optimization into

our focus for system identification and controller design. These identified real time systems and the controller designed for the identified system can be trained as a neural network instead of transfer functions obtained for the identified system and controller in this thesis. We believe this procedure will be beneficial for high order non-linear systems that have no mathematical model available.



REFERENCES

1. **Precision Modular Servo Control Experiments booklet**, 2013., 3-927-Feedback Instruments Ltd., Park Road, Crowborough, East Sussex., United Kingdom.
2. **Bahador R., Milad E., Mohammad R., (2015)**, " *Precise angular speed control of permanent magnet DC motors in presence of high modeling uncertainties via sliding mode observer-based model reference adaptive algorithm*", *Mechatronics* 28 (2015) 79–95.
3. **Sadiq A. A., Bakare G. A., Anene E. C., Mamman H. B., (2013)**, " *A Fuzzy-Based Speed Control of DC Motor Using Combined Armature Voltage and Field Current*" , September 2-4, 2013. Chengdu, China
4. **Wenbin Y., Dada W., Pengfei J., Weiguo L., (2012)**, " *The PWM speed regulation of DC motor based on intelligent control*" , *Systems Engineering Procedia* 3 (2012) 259 – 267.
5. **Premkumar K., Manikandan B.V., (2014)**, " *Adaptive Neuro-Fuzzy Inference System based speed controller for brushless DC motor*" , *Neurocomputing* 138 (2014) 260–270.
6. **Lekhchine S., Bahil T., Aadlia I., Layate Z., Bouzeria H., (2015)**, " *Speed control of doubly fed induction motor*" , *Energy Procedia* 74 (2015) 575 – 586.
7. **Premkumar K., Manikandan B.V., (2015)**, " *Fuzzy PID supervised online ANFIS based speed controller for brushless dc motor*" , *Neurocomputing* 157 (2015) 76–90.
8. **Singh C. P., Kulkarni S., Rana S.C., (2013)**, " *Scientists State-Space Based Simulink Modeling of BLDC Motor and its Speed Control using Fuzzy PID Controller*" , *International Journal of Advances in Engineering Science and Technology*, vol. 2 , no. 3, pp.359-369.

- 9. Azuwien Aida B., WahyuMulyo U., ZainalAlam H., NooradzianieMuhd.Zin, Sy Yi S. , Roslina Mat A., (2013), "Speed Tracking of Indirect Field Oriented Control Induction Motor using Neural Network", *Procedia Technology* 11(2013) 141–146.**
- 10. Tiago H. dos S., Alessandro G., Sergio A. O. da Silva, Marcelo S., (2014), "Scalar control of an induction motor using a neural sensorlesstechnique", *Electric Power Systems Research* 108 (2014) 322– 330.**
- 11. Ehab S. Ali, (2015), "Speed control of induction motor supplied by wind turbine viaImperialist Competitive Algorithm", *Energy* 89 (2015) 593e600.**
- 12. NihatÖ., EmreÇ., (2012), "Speed control of permanent magnet synchronous motors using fuzzy controllerbased on genetic algorithms", *Electrical Power and Energy Systems* 43 (2012) 889–898.**
- 13. Bharat B., Madhusudan S., (2011), "Adaptive control of DC motor using bacterial foraging algorithm", *Applied Soft Computing* 11(2011) 4913–4920.**
- 14. Shaozhong C., Ji T., (2012), "Double Motor Coordinated Control Based on Hybrid Genetic Algorithm and CMAC", *PhysicsProcedia* 33 (2012) 975 – 982.**
- 15. Dušan F., Iztok F., RikoŠ., (2016), "Parameter tuning of PID controller with reactive nature-inspiredalgorithms", *Robotics and Autonomous Systems* 84 (2016) 64–75.**
- 16. Ermira B., Petraq M., (2013), "A Comparison of conventional and nonconventional methods of DC motor speed control", *Prishtina, Kosovo*.**
- 17. Dorf R. C., Bishop R. H., (2005), "Modern Control Systems", Pearson Prentice Hall, United States.**
- 18. Ogata K., (2010), "Modern Control Engineering", PrenticeHall, United States.**



APPENDICES

Curriculum vitae

PERSONAL INFORMATION:

Full Name: Ahmed EmadMahmood
Date of Birth: December^{13th} 1988
Gender: Male
Nationality: Iraqi
Address: turkey-ankara
E-mail: Ahmadalchechany@yahoo.com
Telephone: Personal Mobile 00905319306990
Status: Married

CERTIFICATION:

Diploma in electric power.
B.sc in electric power engineering.
M.sc in electronic and communication in Cankaya University in turkey.

LANGUAGES:

Arabic: native
English
Turkish

COMPUTER SOFTWARE PROGRAMS:

General.
Experience in the use of the Internet.
Microsoft Word, Excel, Access, PowerPoint.
Matlab
Arc GIS(arc map)

Areas of work:

1-Work at kar group for oil and gas in Iraq :-
Amine unit in termination and testing (ESDV),(pcv),(sv),(lv) valves , all receiving and sending devices...cable tray installing in amine site
-Pump station in termination and cable tray.
-Booster pump in termination.
-Loop check and line check for(24)volt DC and(220)volt AC from site to control Room.
-Maintenance of(24)volt DC and(220)volt AC electrical devices in amine unit-pump Station and booster pump.
-Work in taza electrical gas station with Lukoil Company as coordinator

2-Work at Samsung company salilalghazal for 5 months

3-work in Kirkuk industrial high school (Baghdad road)

